ChemMedChem

Research Article
doi.org/10.1002/cmdc.202400937

Chemistry Europe
European Chemical Societies Publishing

www.chemmedchem.org

Elucidating the High Affinity Copper(II) Complexation by the Iron Chelator Deferasirox Provides Therapeutic and Toxicity Insight

Aixa M. Orta Rivera,[a] Luis A. Landrau Correa,[b] Selene L. Schiavone-Chamorro,[a] Moriana Rankins,[a] Mariela V. Pérez Otero,[b] Josué A. Benjamín-Rivera,[a] José A. Vega Aponte,[a] Valerie B. Ebenki,[a] Adriana I. Vargas Figueroa,[a] Andrei V. Astashkin,[c] Lauren Fernández-Vega,*[d] and Arthur D. Tinoco*[a]

Tinoco A-Team Deferasirox (Def), an orally administered iron-chelating drug, has drawn significant interest in repurposing for anticancer application due to the elevated Fe demand by cancer cells. But there are also concerns about its severe off target health effects. Herein Cu(II) binding is studied as a potential off target interaction. The aqueous solution stability and speciation of the ternary complex Cu(Def)(pyridine) was studied by UV-Vis and EPR spectroscopy, ESI-mass spectrometry, and cyclic voltammetry under physiologically relevant conditions. The complex is observed to be a redox active, mononuclear Cu(II) complex in square planar geometry. UV-Vis spectroscopy demonstrates that at pH 7.4 the complex is quite stable ($\varepsilon_{337nm} = 10{,}820\ M^{-1}cm^{-1}$) with a log $K = 16.65 \pm 0.1$. Cu scavenging from the Cu transporters ceruloplasmin and albumin was also studied. Def does not inhibit ceruloplasmin activity but forms a ternary Cu(II) complex at the bovine serum albumin ATCUN site. Cu(Def)(py) displays potent but nonselective cytotoxicity against A549 cancer and MRC-5 noncancer lung cells but the potency of the ternary protein complex was more moderate. This work elucidates potential Def toxicity from Cu complexation in the body but also cytotoxic synergy between the metal and chelator that informs on new drug design directions.

1. Introduction■Dear Author, please check numbering of the headlines■

Deferasirox (Def; also referred to as DFX) is a very high affinity iron(III) chelator that is widely used to treat patients of chronic iron overload due to blood transfusions (ages 2 or older) and due to non-transfusion-dependent thalassemia (ages 10 or older). Commercially known as Exjade, it was approved by the US FDA in 2005 and, to date, is the only orally administered Fe chelator in the US. Deferasirox has recently been considered for drug repurposing as an anticancer agent given the high Fe demand exhibited by cancer cells relative to noncancer cells. In studies examining the cytotoxic effect of the compound in metal-free form[1,2] or as a noniron metal complex for intracellular iron-dependent transmetalation,[3,4] Def displays promising anticancer features although it lacks cancer cell selectivity.

Off target effects of Def have been a source of controversy regarding its use due to its toxicity and elevated cases of fatality.[5,6] It is packaged with FDA boxed warnings.[7,8] Hall et al. has found that in kidney cells Def causes mitochondrial swelling without depolarization or opening of the mitochondrial permeability transition pore, which may be the source of its nephrotoxicity in humans.[8] This toxicity can be ameliorated with Def complexed with Fe(III),[8] generating the $Fe(Def)_2$ species.[9]

Off target effects is the inspiration for this study to examine the copper(II) binding by Def. As a chelator, Def is a tridentate ONO hard Lewis base which binds hard Lewis acids like Fe(III) and Ti(IV) with very high, comparable affinity in 1:2 metal:ligand meridional modality (log K~39).[4] Recently we reported on Cu(II) complexation by Def in a 1:1 stoichiometry and the lack of antimicrobial activity by the compound at mid micromolar concentration,[10] which may be owed to the seemingly higher affinity of Def for Cu(II), an intermediate Lewis acid, than previously indicated.[11] The compound is quite water insoluble (probably owed to dimerization or higher nuclearity complexation) but can be solubilized in pyridine, which was a required co-solvent for the antimicrobial studies. Ebrahimipour et al. obtained a crystal structure of the heteroleptic complex Cu(Def)(py) in which the Cu(II) is bound by pyridine in monodentate modality and by Def in tridentate modality, forming a square planar geometry.[12] The solubilization of the Cu(Def)

[a] A. M. Orta Rivera, S. L. Schiavone-Chamorro, M. Rankins, J. A. Benjamín-Rivera, J. A. Vega Aponte, V. B. Ebenki, A. I. Vargas Figueroa, A. D. Tinoco
Department of Chemistry, University of Puerto Rico, Río Piedras Campus, Río Piedras, Puerto Rico 00925-2537, United States
E-mail: arthur.tinoco@upr.edu

[b] L. A. Landrau Correa, M. V. Pérez Otero
Department of Biology, University of Puerto Rico, Río Piedras Campus, Río Piedras, Puerto Rico 00925-2537, United States

[c] A. V. Astashkin
Department of Chemistry and Biochemistry, The University of Arizona, Tucson, AZ 85721-0041, United States

[d] L. Fernández-Vega
Division of Science, Technology, and Environment, University Ana G. Méndez-Cupey Campus, 1399 Av. Ana G. Méndez, San Juan, PR 00926, United States
E-mail: lafernandez@uagm.edu

Supporting information for this article is available on the WWW under https://doi.org/10.1002/cmdc.202400937

complex that we noted in pyridine in our earlier study[10] was apparently induced by solvent coordination.

Herein the solution speciation and stability of the Cu-(Def)(py) complex was studied by UV-Vis spectroscopy and EPR at physiologically relevant pH. The complex was found to remain intact at pH 7.4 at micromolar concentrations. Its cytotoxicity was examined against the lung cancer A549 cell line and noncancer MRC5 cell line to assess cell death capability and general toxicity and was compared with the activity of metal-free Def. Given the potent cytotoxicity of the Cu(Def)(py) complex, even higher than Def, the Cu(II) scavenging ability of Def was studied with the main Cu blood transport proteins ceruloplasmin and albumin to determine whether Cu scavenging is a possible source of off target toxicity of the chelator. This work sheds new light on the chelator medicinal functionality of Def and elucidates how Cu(II) binding could facilitate additional potential anticancer therapeutic use.

2. Results and Discussion

2.1. Insights Into the Aqueous Speciation and Solution Stability of Cu(Def)(py) at pH 7.4

The compound Cu(Def)(py) was synthesized by preparing a Cu(II) Def compound in a 50:50 methanol:water solvent mixture from the reaction of $CuCl_2$ (aq) with our own synthesized Def (^{1}H NMR; Figure S1).[10] A green product precipitates from solution and after washing extensively with H_2O, it was dissolved in pyridine and then isolated by rotovap. The emerald green product that is obtained is poorly soluble in water, DMSO, DMF, and most other solvents but is quite soluble in pyridine. The elemental analysis suggests a molecular formulation of [Cu(Def)(py)]·Pyridine·0.5 H_2O although it is unclear if a true mononuclear or higher nuclearity metal species with the same stoichiometric ratio of metal, ligands, and solvates is obtained in solid state. The FT-IR spectrum for the compound reveals characteristic bands for the presence of deferasirox (ν(C=O) 1699, 1599; ν(C–O) 1263,1236 cm^{-1}) (Figure S2).

Once the Cu(Def)(py) compound is dissolved in pyridine, the solution can be diluted in water without precipitation of the compound. Millimolar concentrations of the compound in a 50:50 H_2O:Pyridine (v/v) solvent mixture remain in solution indefinitely.

The UV Vis spectrum for these solutions reveal an absorbance maximum at 335 nm with an extinction coefficient of 11,430 $M^{-1}cm^{-1}$, characteristic of a ligand to metal charge transfer (LMCT) band. An EPR spectrum of the compound in 50:50 H_2O:pyridine (Figure 1a and Figure S3) is typical for a mononuclear Cu(II) complex. It is characterized by a slightly rhombic g-tensor with ($g_\perp$, $g_{||}$ = 2.05, 2.26) and near-axial hyperfine interaction (hfi) of the Cu nucleus with ($A_\perp$, $A_{||}$ = ~0,471.0 MHz). The observed combination of $g_{||}$ and $A_{||}$ values agrees with those expected for square planar Cu(II) complexes featuring two nitrogen and two oxygen ligands due to monodentate N-coordination by the pyridine and O,N,O tridentate coordination by Def.[13] The presence of (at least) two

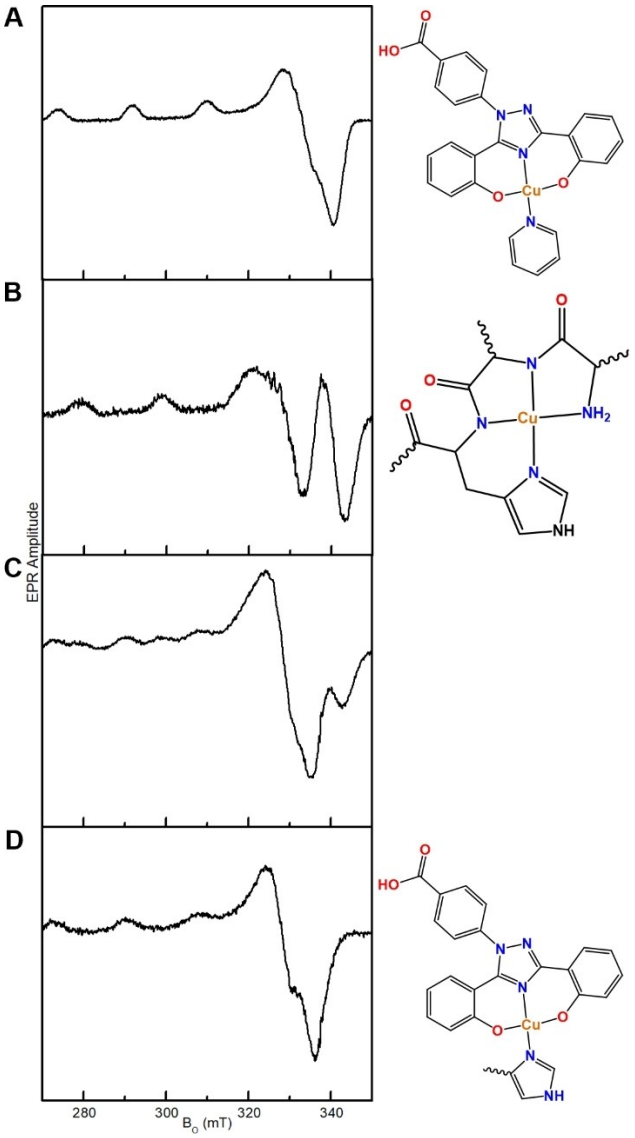

Figure 1. EPR spectra of Cu(II) complexes and the proposed coordination structures. (A) The Cu(Def)(py) EPR spectrum was collected in frozen pyridine/water 50:50 (v/v) solution. Experimental conditions: microwave frequency, 9.463 GHz; microwave power, 200 mW; magnetic field modulation amplitude, 0.2 mT; temperature, 77 K. (B) The EPR spectrum of Cu(II)-bound BSA, in which Cu(II) is coordinated at the ATCUN site. (C) The EPR spectrum of the reaction mixture of Cu(II)-bound BSA and Def. (D) The processed EPR spectrum of the reaction mixture of Cu(II)-bound BSA and Def after subtracting out the signal for residual Cu(II)-bound BSA. The resultant spectrum appears to depict a ternary Cu(BSA)(py) complex. All protein samples were prepared in frozen 50:50 (v/v) 20 mM HEPES (pH 7.4; 0.1 M NaCl):glycerol. Experimental conditions for BSA samples were similar to that of Cu(Def)(py) except that the microwave frequency was 9.443 GHz.

coordinated nitrogens is supported by the poorly resolved hyperfine structure of about five lines observed at $g_\perp$, with the splitting between these lines at about 17.0 mT. A square planar geometry was observed for Cu(Def)(py) in solid state for a previously published X-ray crystal structure.[12] An electrospray ionization mass spectrum was collected of 1 ppm compound diluted in water to yield 0.05% pyridine (v/v) to which ammonia was added to a final 1% (v/v) (Figure S4). The MS reveals a base peak at 514.08 m/z indicative of a mononuclear Cu(Def)(py)

species ($C_{26}H_{18}N_4O_4Cu+H^+$ adduct) and also a peak at 871.06 m/z for a dimeric species $[Cu(Def)]_2$ ($C_{42}H_{26}N_6O_8Cu_2+H^+$ adduct), in which no solvent molecule is coordinated.

A solution stability study was performed to examine the stability of micromolar concentration of Cu(Def)(py) in high water content by UV Vis spectroscopy.Two 40 μM Cu(Def)(py) solutions were prepared containing 2% pyridine (v/v) in either pure water or in 5 mM ammonium bicarbonate buffer (pH 7.4) and they were monitored over time for up to 72 h. The pyridine/water solution revealed the LMCT band at $\lambda_{max}=$ 335 nm ($\varepsilon=10{,}910\ M^{-1}cm^{-1}$) and the pyridine/buffer solution had the LMCT band at $\lambda_{max}=337$ nm ($\varepsilon=10{,}820\ M^{-1}cm^{-1}$) (Figure S5). Both solutions were extremely stable, showing virtually no change in absorbance during the experiment.

A spectrophotometric metal ligand complexation experiment was performed at pH 7.4 with a 0.1 M ionic strength to determine the stability constant for Cu(Def)(py). An in situ solution of $Cu(py)_4$ was prepared[14,15] and it was used to make separate solutions of 50 μM $Cu(py)_4$ reacted with different mole equivalents of Def (up to 7.5 mole equivalents) in a solvent mixture containing 50% pyridine (v/v), 2.5% DMF (v/v) in 20 mM HEPES buffer (0.1 M NaCl, pH 7.4). The solutions were equilibrated for 24 h at RT and then their UV Vis spectra were recorded. The absorbance corresponding to the LMCT band for Cu(Def)(py) was the only feature present in the wavelength range greater than 320 nm. A saturation curve (Figure S6) was generated from the absorbance at 346 nm after accounting for all equilibria in solution as follows:

K

$$Cu(py)_4^{2+}+H_2Def^{1-}\rightleftharpoons Cu(Def)(py)^-+3\ py+2H^+$$

$$K=\frac{[Cu(Def)(py)^-][H^+]^2}{[Cu(py)_4^{2+}][H_2Def^{1-}]} \quad (1)$$

$$K=K_{app}[H^+]^2 \quad (2)$$

where K_{app} is an apparent binding constant and is represented by Equation (3).

$$K_{app}=\frac{[Cu(Def)(py)^-]_{eq}}{[Cu(py)_4^{2+}]_{eq}[H_2Def^{1-}]_{eq}} \quad (3)$$

The total Cu(II) concentration is defined by $[Cu(py)_4^{2+}]_{initial}$ and it is represented by the mass balance of all Cu(II) species at equilibrium (Equation (4)).

$$[Cu(py)4^{2+}]_{int}=[Cu(py)_4^{2+}]_{eq}+[Cu(Def)(py)^{1-}]_{eq} \quad (4)$$

Equation (4) is rearranged in terms of $[Cu(py)_4^{2+}]_{eq}$ to yield Equation (5).

$$[Cu(py)4^{2+}]_{eq}=[Cu(py)4^{2+}]_{int}-[Cu(Def)(py)^{1-}]_{eq} \quad (5)$$

The total mass balance of H_2Def^{1-} is represented by Equation (6)

$$[H_2Def^{1-}]_{int}=[H_2Def^{1-}]_{eq}+[Cu(Def)(py)^{1-}]_{eq} \quad (6)$$

Equation (6) is rearranged in terms of $[H_2Def^{1-}]_{eq}$ to give Equation (7).

$$[H_2Def^{1-}]_{eq}=[H_2Def^{1-}]_{int}-[Cu(Def)(Py)^{1-}]_{eq} \quad (7)$$

Equation (5) is substituted into Equation (3) to obtain Equation (8).

$$K_{app}=\frac{[Cu(Def)(py)^{1-}]_{eq}}{\left[[Cu(py)_4^{2+}]_{int}-[Cu(Def)(py)^{1-}]_{eq}\right][H_2Def^{1-}]_{eq}} \quad (8)$$

Finally Equation (8) is rearranged to Equation (9).

$$[Cu(Def)(py)^{1-}]_{eq}=\frac{K_{app}{}^*[Cu(py)4^{2+}]_{int}{}^*[H_2Def^{1-}]_{eq}}{K_{app}{}^*[H_2Def^{1-}]_{eq}+1} \quad (9)$$

Equation (9) can be simplified to Equation (10).

$$y=\frac{K_{app}{}^*[Cu(py)_4{}^{2+}]_{int}{}^*X}{K_{app}{}^*x+1} \quad (10)$$

where $x=[H_2Def^{1-}]_{eq}$ and $y=[Cu(Def)(py)^{1-}]_{eq}$

$[Cu(py)_4{}^{2+}]_{int}=50\ \mu M$

A plot of $[Cu(Def)(py)_4{}^{1-}]_{eq}$ vs $[H_2Def^{1-}]_{eq}$ was generated according to Equation (10) to determine the value of K_{app} (Figure 2). The concentration of $[Cu(Def)(py)_4{}^{1-}]_{eq}$ was derived from the absorbance at 346 nm ($\varepsilon=12{,}300\ M^{-1}cm^{-1}$) and the concentration of $[H_2Def^{1-}]$ was then determined by mass balance. Equation (10) was iteratively fitted by nonlinear analysis using OriginPro8.5 and developing a User Defined equation. The K_{app} value was determined to be $(2.14\pm0.20)\times10^5\ M^{-1}$. The value of K (Equation (2)) was then determined at pH 7.4.

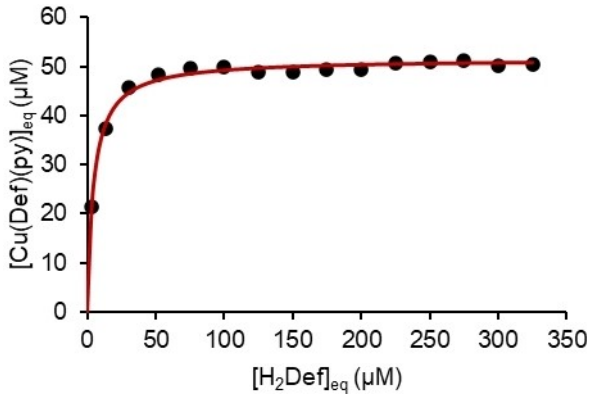

Figure 2. Saturation curve for the determination of the formation constant for Cu(Def)py derived from the equilibria concentrations of $[Cu(py)_4{}^{2+}]_{eq}$ and $[H_2Def]_{eq}$ after the addition of different mole equivalents of Def. Equation (10) was iteratively fitted by nonlinear analysis using OriginPro8.5. The K_{app} value was determined to be $(2.14\pm0.20)\times10^5\ M^{-1}$.

$$K = (2.14 \times 10^5\ M^{-1}) \times (3.98 \times 10^{<M->8}M)^2 = 3.39 \times 10^{<M->10}M$$

$$\log K = -9.62$$

After accounting for all other equilibria (Table 1), the stability constant of Cu(Def)(py) was determined to be log K = 16.65 ± 0.1 M^{-2}. The affinity of deferasirox for Cu(II) is sufficiently high to suggest that it may possess the capacity to scavenge biologically coordinated Cu(II).

Cyclic voltammetry measurements were performed to determine the redox capacity of Cu(II) when coordinated to Def. This experiment proved challenging due to solubility limits of Cu(Def)(py). The blank solution (25% pyridine (v/v):75% 500 mM KCl (aq), pH = 7.4) exhibited a semireversible redox process with a $E_{pc} = -0.515$ V and $E_{pa} = -0.417$ V vs NHE (Figure S7; the different redox events are labeled by numbers) owed to the absorption(1)/desorption(2) of pyridine on the electrode surface.[16,17] The CV of $Cu(py)_4^{2+}$ reveals a reduction event (5) at $E_{pc} = -0.37$ V and an oxidation event (3) at $E_{pa} = -0.16$ V, which may be attributed to the one electron Cu(II) reduction and Cu(I) oxidation while coordinated to the py ligands. The CV of Cu(Def)(py) reveals a reduction event (6) at $E_{pc} = -0.47$ V and an oxidation event (3) at $E_{pa} = -0.16$ V. The reduction event may be the one electron reduction of Cu(II)(Def)(py). This process appears to be irreversible possibly due to significantly weaker affinity of Def for Cu(I) resulting in dissociation of the chelator. The oxidation event that follows matches the one observed for the $Cu(py)_4$ sample and thus could be the one electron oxidation of $Cu(I)(py)_4$. The reduction and oxidation events are written as follows:

$$Cu(II)(Def)(py) + e^- \rightarrow Cu(I)(Def)(py)$$

$$\rightarrow Cu(I)(py)_4 + H_2Def$$

$$\rightarrow Cu(II)(py)_4 + e^-$$

Neither the CV of $Cu(py)_4^{2+}$ nor Cu(Def)(py) exhibit the absorption/desorption of pyridine as observed in the blank run. The reduction potential of Cu(Def)(py) is within the biological redox window of +0.8 to −0.5 V, which suggests that it would be likely to be reduced within the cellular environment, resulting in dissociation of the chelator.

Table 1. All of the equilibria involved in the determination of the formation constant for Cu(Def)(py).

Equilibria	log K	Ref.
$Cu(py)_4^{2+} + H_2Def^{1-} \rightleftarrows Cu(Def)(py)^- + 3py + 2H^+$	−9.62	
$Cu(II) + 4py \rightleftarrows Cu(py)_4^{2+}$	6.71	[15]
$Def^{3-} + 2H^+ \rightleftarrows H_2Def^-$	19.41	[11]
$Cu(II) + py + Def^{3-} \rightleftarrows Cu(Def)(py)^-$	16.65 ± 0.1	

2.2. Examining the Potential of Def to Scavenge Cu from the Cu Transporter Proteins Ceruloplasmin and Serum Albumin

Cu is an essential and highly redox active metal that partakes in a number of enzymatic processes involving electron transfer. The metal plays an Fe regulatory role in multi-copper ferroxidases, which convert Fe(II) to Fe(III) and facilitate Fe mobility through the body.[18] A fascinating detail about Cu is that while vital to human life, it is quite toxic and thus it is highly regulated. It exists in protein bound form at high affinity sites in serum and within cells. In human serum, Cu is present at ~20 μM. Three proteins are attributed to Cu handling in serum: ceruloplasmin, serum albumin, and transcuprein.[19] Ceruloplasmin transports 40–70% of total blood Cu whereas albumin accounts for 10–15%, and transcuprein (alpha-2-macroglobulin) accounts for 5–15%. Given the relatively high affinity of deferasirox for Cu(II), we were interested in studying whether it could scavenge Cu from the blood transporter proteins. For this study, we focused specifically on ceruloplasmin and albumin as representatives of Cu nonexchangeable and exchangeable proteins, respectively.

2.3. Ceruloplasmin

In its Cu-bound form, ceruloplasmin is a multifunctional enzyme, with its best-known function as a multi-copper ferroxidase. Structurally, it consists of six domains and between 6–8 Cu ions (PDB: 2 J5 W).[20] Cu coordination within the enzyme consists of the classical Cu Types 1 through 3 modality. It is mainly characterized by an active site containing a trinuclear Cu cluster (two type 3 Cu bound by a dioxo group) and a proximal Cu (Type 2) with a distance of 12–13 Å from the cluster that catalyzes ferrous oxidation. The other single Cu atoms are type 1 and located in the even-numbered domains.[20] It is estimated that about half of the copper oxidation states are Cu(I) and Cu(II),[21] in which the active site cycles the oxidation state from Cu(I), when the O_2 substrate binds, to Cu(II) after oxygen (O_2) cleavage.[22] The overall process promotes the 4-electron reduction of O_2.[22]

Ceruloplasmin is classified as a non-exchangeable Cu transporter because it does not readily exchange Cu with other proteins or chelators in blood but instead releases Cu to cells via receptor-mediated processes.[19] An activity-based approach was taken to determine whether Def is able to inhibit the enzymatic activity of ceruloplasmin, presumably by Cu scavenging. A colorimetric assay kit was used by employing N, N-dimethyl-p-phenylenediamine as substrate, which becomes colored (absorbance at 560 nm) when oxidized by ceruloplasmin. Human ceruloplasmin was commercially obtained and this protein source contained 5–6 Cu ions. KCN was included in the assay as a negative control given its known property as an inhibitor of ceruloplasmin.[23] Autoabsorbance of the substrate was examined by running all experiments with and without ceruloplasmin, and no autoabsorbance was observed (Figure 3). In addition, a set of experiments were run without the presence of substrate to rule out any background activity. Cu(Def)(py)

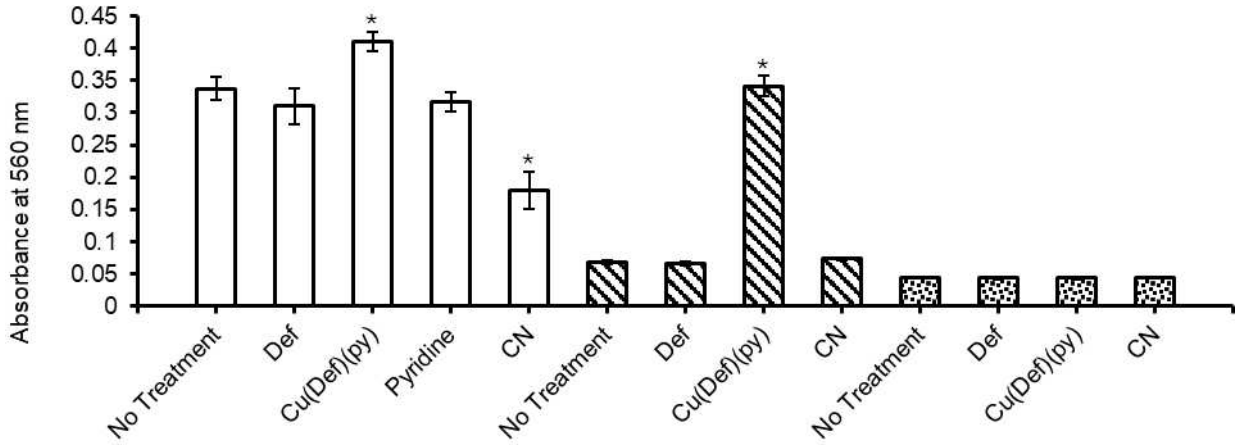

Figure 3. A colorimetric-based ceruloplasmin activity assay was used to determine the enzyme inhibitory behavior of Cu(Def)(py). The absorbance at 560 nm was recorded for the oxidation of the substrate. The samples were measured in three different ways to ensure activity observed came from the enzyme. Samples contain enzyme and substrate (no pattern), substrate only (line pattern), or enzyme only (circle pattern). The corresponding samples contain 1000 mU/mL ceruloplasmin and 100 μM deferasirox, 100 μM Cu(Def)(py),10 μM cyanide (CN), or no treatment. Background conditions for Cu(Def)(py) and pyridine samples: 2.5% pyridine and 97.5% 1X assay buffer; for all other samples: 2.5% water, 2.5% DMF, and 95% 1X assay buffer. Results are shown as mean ± SD of quadruplicates.*, p-value < 0.05.

was included in this study as a representation of the Cu(II) complexation product that could form due to Def scavenging Cu from the enzyme. It was observed that Def was ineffective at inhibiting the enzyme. Interestingly, Cu(Def)(py) was able to cause the oxidation of the substrate in the absence of the enzyme, and in the presence of the enzyme the absorbance intensity was slightly higher than with the enzyme alone. This finding further reveals that Cu(Def)(py) is a redox active compound and demonstrates that Def does not pull Cu from the enzyme.

2.4. Albumin

In blood serum, albumin is the most abundant protein at ~600 μM. Due to the presence of numerous binding sites, it is able to bind a wide diversity of hydrophobic and hydrophilic species, serving as a transporter of many of them. Fatty acids, which would otherwise be insoluble in blood,[24] are bound at up to seven sites in albumin to be biodistributed throughout the body. Albumin plays the crucial role of delivering Cu(II) to cells, in particular to the liver and kidney.[25] Very importantly, it facilitates extracellular defense against free Cu(I/II) ions that could lead to the production of uncontrolled amounts of reactive oxygen species.[19] Its high affinity Cu(II) site (log K = 13.02)[26] is normally only 0.03% occupied, allowing for abundant sites to capture excess Cu entering the blood stream.[19] This high affinity site is a classical amino-terminal copper and nickel (ATCUN) metal binding site (Figure S8a). ATCUN sites consist of the N-terminal amine, the first two deprotonated amides, and the third amino acid His imidazole. The amino-terminal end of albumin is unstructured, making the ATCUN site highly solvent exposed, which likely explains why it is a Cu exchangeable site.

Due to the higher stability constant of Cu(Def)(py) than that of the albumin Cu(II)-ATCUN, it was anticipated that Def would be able to scavenge Cu(II) from the protein. To evaluate this possibility, studies were performed with bovine serum albumin, which features 80% sequence homology with the human protein and the Asp-Thr-His ATCUN site (the human site is Asp-Ala-His). Cu(II)-bound BSA was prepared by the stoichiometric addition of Cu(II) from $CuCl_2$ to the protein. Cu(II) binding does not produce a distinctive change in the protein UV Vis spectrum at micromolar concentrations. To validate the formation of the Cu(II) ATCUN adduct, an EPR spectrum was collected at pH 7.4. The spectrum (Figure 1B) displays a g-tensor with ($g_{\perp}$, $g_{||} = 1.98$, 2.18), which is typical for a mononuclear Cu(II) complex bound to the ATCUN site[27] where ($g_{||} = 2.18–2.19$) in peptides containing Cu(II) bound to His-3 in the ATCUN sites. The spectrum also shows a poorly resolved near-axial hfi interaction with ($A_{\perp}$, $A_{||} = \sim 0$, 607.4 MHz). When mid-micromolar Cu(II)-bound BSA is reacted with equimolar amounts of Def at pH 7.4, a new absorbance rapidly appears at 340 nm with an extinction coefficient of 12,010 $M^{-1}cm^{-1}$ (a value confirmed by a Def titration study; Figures S9 and S10). Monitoring this reaction with 61.3 μM Cu(II)-bound BSA by UV-Vis showed virtually 100% conversion to the product within the first five minutes of the reaction (Figure 4). This product is distinct from the Cu(II) species that forms when Def is added to $Cu(Tris)_4$ in the buffered solution (Figure 4), which is a green species that rapidly precipitates from solution, which is presumably the very poorly water soluble Cu(II) Def species that we previously synthesized in water.[10]

After completing the reaction of Cu(II)-bound BSA with Def, the protein was extensively buffer washed by rapid spin dialysis and the UV-Vis spectrum revealed the presence of the absorbance at 340 nm, with no apparent dissociation as validated by quantifying the protein content by the Bradford assay and the Cu content by the ferrozine assay. To evaluate

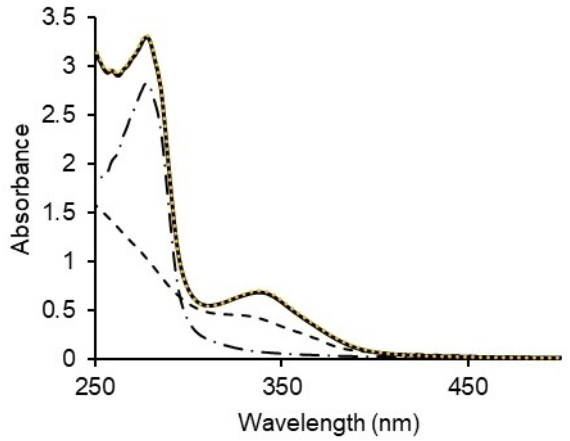

Figure 4. UV-Vis absorbance spectra of Cu(II)-bound BSA (dash dot line), Cu(II)-bound BSA in reaction with equimolar Def (black line for after five minutes; Orange dotted line for after 24 hours), and Cu(II) in reaction with equimolar Def (black dotted line; after five minutes of reaction) at pH 7.4. The $Cu(Tris)_4$ reaction with equimolar Def was also monitored (dashed lines; after five minutes). The concentration of all of these samples was 61.3 μM.

the coordination of the Cu species by EPR, the protein was concentrated and an 815 μM sample was obtained. The spectrum reveals the presence of two species (Figure 1c). One of the species is of the Cu(II) ATCUN adduct, accounting for 30% of the total spectrum. After subtracting this species from the spectrum, a new Cu(II) species was apparent (Figure 1d), which accounts for the remaining 70% of the spectrum and thus is the dominant species. The EPR spectrum of this species is comparable with that of Cu(Def)(py), in which a mononuclear square planar Cu(II) species shows 2 O and 2 N bonds. It is characterized by a slightly axial g-tensor with $(g_{\perp}, g_{||}) = (2.05, 2.26)$ and the poorly resolved near-axial hfi interaction of the Cu nucleus with $(A_{\perp}, A_{||}) = (\sim 0, 497.2)$ MHz. The observed combination of $g_{||}$ and $A_{||}$ values also agrees with those expected for square planar copper complexes featuring two N and two O ligands.[13] These findings suggest that the Cu(II) species that formed is a Cu(BSA)(Def) ternary complex in which the His3 residue of the ATCUN site remains bound to the Cu(II) and the Def is bound in O,N,O tridentate modality (Figure 1d; Figure S8b). The UV-Vis spectra of the Cu(BSA)(Def) ternary complex is similar but not identical to that of Cu(Def)(py) (Figure S10). At the high micromolar concentration obtained after concentrating the protein sample, it appears as though there is some repartitioning of the Cu(II), leading to 30% of it being exclusively bound to the ATCUN site. This results provides insight into the relative Cu(II) affinity by the ATCUN site and within the ternary complexation.

Ternary complexation of Cu(II) at the ATCUN site of albumin was also observed for triapine,[28] an iron chelator specifically designed as an anticancer agent.[29] The Cu(II) coordination is comparable to what is observed for Def with the His residue as the sole protein bond and tridentate N,N,S coordination by triapine in a square planar geometry.[28]

When performing the reaction of Cu(II)-bound BSA with Def at 500 μM concentration of both reactants, a green precipitate immediately formed that was visible to the eye and no absorbance was observed at 340 nm. After the protein from this reaction was extensively buffer washed, it was analyzed by EPR. Interestingly, the EPR spectrum was characteristic of just the Cu(II) ATCUN adduct (Figure S11), with a 45% reduction of the adduct relative to the EPR spectrum collected for Cu(II)-bound BSA. These results suggest that at high micromolar concentrations, the reaction with Def is kinetically driven, leading to Def scavenging Cu(II) from the protein (at least partially) and no formation of a ternary complex. The green precipitate that was observed to form was likely the Cu(II) Def species that we previously synthesized in water.[10]

2.5. Comparing the Antiproliferative/cytotoxic behavior of Def and Cu(II) Def Complexes

The compounds Def and Cu(Def)(py) were sent to the NCI 60 human tumor cell line anticancer drug screen. The cell lines represent nine human cancers: leukemia, melanoma, lung, colon, central nervous system, ovarian, renal, prostate, and breast cancers. An initial screening is done by performing a one-dose test of 10 μM of the compounds administered for 72 h. At this concentration, Def is able to inhibit the growth of all the cell lines by an average 67.5% (Table 2). Unfortunately the data collected for Cu(Def)(py) were not very useful because the sample was tested under solvent conditions (using DMSO to prepare the initial stock instead of our recommendation of pyridine) not suitable for solubilizing the compound. This very low solubility resulted in poor potency against the cell lines (Table S1). A rescreening of the compound is not possible given that pyridine is considered by the screening facility as hazardous/volatile.

The antiproliferative/cytotoxic potency of Cu(Def)(py) was examined under solution conditions at pH 7.4 that are suitable for cell growth and that maintain the compound soluble and stable. The compound was tested against the human lung cancer cell line A549 and noncancer cell line MRC-5 and cell viability after 72 h treatment was measured by the MTT colorimetric assay (Figure 5). The compound exhibits an IC_{50} value against A549 of 1.8 ± 0.2 μM and results in total loss of

Table 2. A summary of the NCI 60 cancer cell line viability screen against 10 μM of Deferasirox for 72 h. The data were calculated as the mean per cell line type.

Cancer Cell Line Type	% Mean Cell Growth
Leukemia	−0.150
Non-Small Cell Lung	35.4
Colon	21.8
CNS	45.5
Melanoma	36.4
Ovarian	36.4
Renal	36.1
Prostate	42.2
Breast	41.7

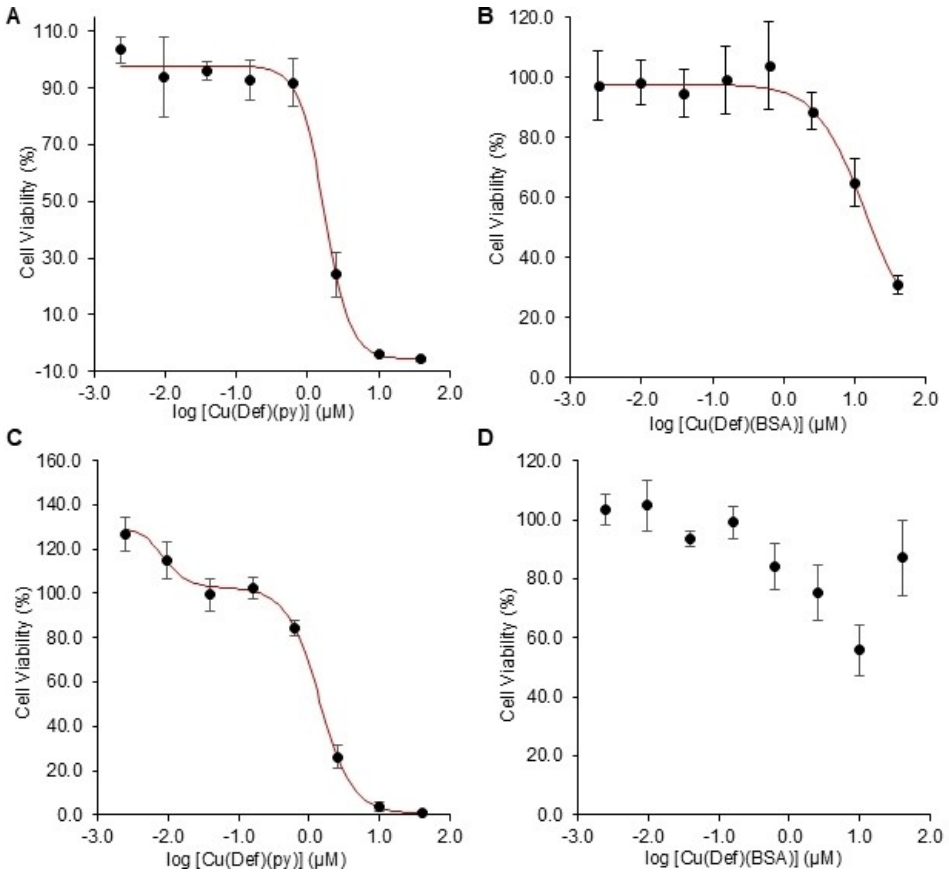

Figure 5. MTT colorimetric assays to measure the cell viability of A549 and MRC-5 cells when treated with different concentrations of the Cu(II) complexes. (A) A549 cell dose-response curve for treatment with Cu(Def)(py) ($IC_{50} = 1.8 \pm 0.2$ μM). (B) A549 cell dose-response curve for treatment with Cu(BSA)(Def) ($IC_{50} = 14 \pm 5$ μM). (C) MRC-5 cell dose-response curve for treatment with Cu(Def)(py). The curve was fitted with a biphasic pharmacological behavior. IC_{50} value 1.4 ± 0.4 μM for antiproliferative behavior and 8.7 ± 0.5 nM for proliferative behavior. (D) MRC-5 cell dose-response curve for treatment with Cu(BSA)(Def). The curve could not be fitted but an approximate IC_{50} value of 10 μM was determined.

viable cells at 10 μM. Interestingly, at concentrations below 0.1 μM, the compound induces proliferation of the MRC-5 cells. Above this concentration, the compound exhibits an antiproliferative/cytotoxic behavior, with an IC_{50} value of 1.4 ± 0.4 μM and total loss of viable cells at 10 μM. The compound exhibits no cancer selectivity unlike the metal-free ligand against the same cell lines; $IC_{50} = 12.1$ μM for A549 and no observable inhibition in MRC-5 cell growth even up to 100 μM concentration.[3] Nonetheless, Cu(Def)(py) is far more toxic than the metal-free ligand. This higher toxicity is likely owed to the presence of the Cu(II), especially given the loss of cell line selectivity.

Previously it was determined that Def can induce the cell death pathway caspase-3 dependent apoptosis in A549 cells[3] and so we wanted to determine whether Cu(Def)(py) could also induce this form of cell death. In addition, the ability of both Def and Cu(Def)(py) to induce the iron-dependent cell death pathway ferroptosis (which sees highly redox intracellular Fe species generating lipid peroxidation) was also examined. To determine caspase-3 dependent apoptosis and ferroptosis induction, an inhibitor-based approach was taken using the MTT cell viability assay. For this study, Q-VD-OPh (caspase-3 dependent apoptosis inhibitor) and Ferrostatin-1 (Fer-1; ferroptosis inhibitor) were used (Figure 6). Cisplatin, a caspase-3 dependent apoptosis inducer, and erastin, a ferroptosis inducer, were included as positive controls. Cisplatin, erastin, Def, and Cu(Def)(py) were treated against A549 for 72 h at roughly IC_{80} concentration values. These concentrations were selected to be able to observe close to maximal potency without eliminating all viable cells. In the presence of Q-VD-OPh, both Def and Cu(Def)(py) exhibited decreased antiproliferative behavior like cisplatin, indicating that they operate by inducing apoptosis. The cells were 2.4 (Def treated) and 2.6 (Cu(Def)(py) treated) times more viable relative to treatment with the compounds without the inhibitor. However, in the presence of erastin, neither Def nor Cu(Def)(py) shows a change in their effect on cell viability, suggesting that they do not induce ferroptosis. It was hard to predict whether Def or Cu(Def)(py) (following likely intracellular dissociation of Def due to the reduction environment) would induce ferroptosis given that the chelator has been observed to inhibit ferroptosis in cardiomyocytes[30] but induce ferroptosis in acute lymphoblastic leukemia cells.[2] A mitochondrially targeted deferasirox derivative (containing a linker with a triphenylphosphonium moiety) could induce ferroptosis in breast cancer cells.[31] It is unclear how exactly Def could induce ferroptosis. The thermodynamic Fe chelation

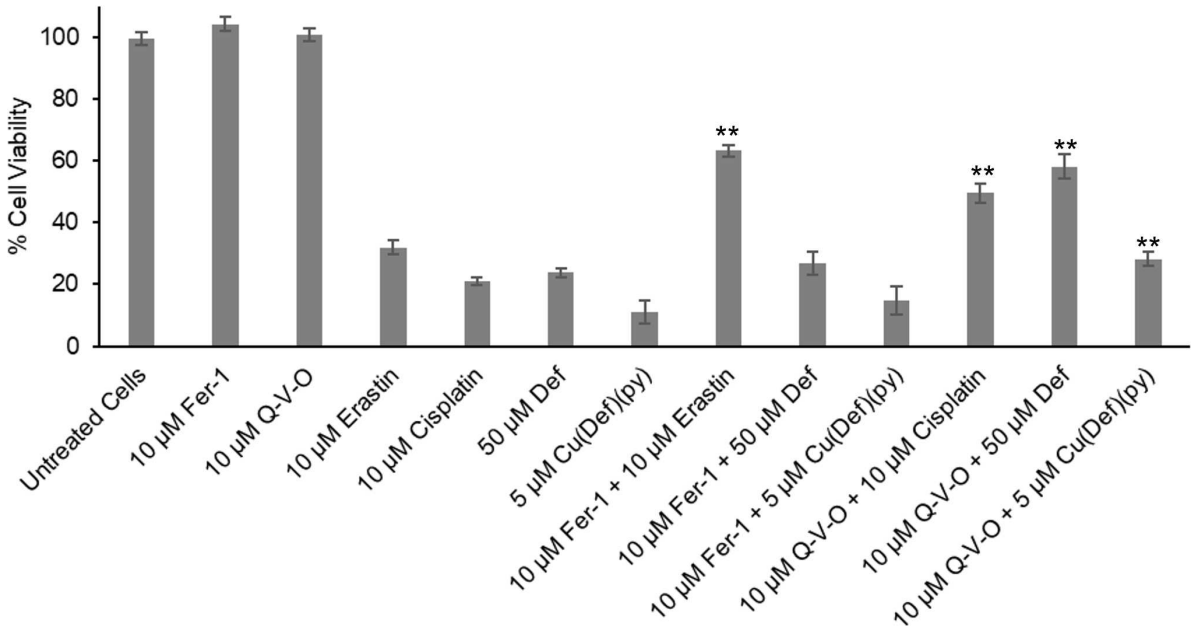

Figure 6. Observed changes in the % cell viability of A549 cells. The cells were pretreated for 2 h with 10 μM Q-VD-OPh (Q–V-O), 10 μM Ferrostatin-1 (Fer-1), or 1X PBS and then treated for 72 h with 50 μM Def, 5 μM Cu(Def)(py), 10 μM erastin, 10 μM cisplatin, or buffer alone. **p-value < 0.01 vs the corresponding treatment without the inhibitor.

product $Fe(Def)_2$ exhibits a low reduction potential ($E_{1/2} = -0.59$ V vs NHE)[4] that would be redox inert if it forms intracellularly, even with the reducing intracellular environment. Kontoghiorghes et al. showed that Def prevents Fe(III) and Cu(II) from causing the lipid peroxidation of linoleic acid.[32] Lipid peroxidation is a hallmark of ferroptosis. Ferroptosis might occur if under certain cellular conditions an Fe monodeferasirox species forms as the dominant intracellular Fe species. Such a species may be more redox active than $Fe(Def)_2$ based on the reduction potentials we have measured.[4] Molecular-based mechanistic studies are warranted to understand the cytotoxic behavior Cu(Def)(py) and why it is far more potent than the metal-free ligand.

The antiproliferative/cytotoxic behavior of the ternary complex Cu(Def)(BSA) was also examined against the A549 and MRC-5 cell lines to determine if the extracellular generation of such a species could be toxic. The ternary complex does exhibit an antiproliferative effect against both cell lines; $IC_{50} = 14 \pm 5$ μM against A549 cells and estimated IC_{50} value of 10 μM against MRC-5. The potency against these cell lines is significantly lesser than the activity of Cu(Def)(py) and up to 100 μM (the highest dosage tested) the ternary complex is unable to fully inhibit proliferation of the cells, reaching ~70% and ~50% inhibition of A549 and MRC-5 cells, respectively. By retaining partial coordination of the Cu(II) in the ternary complex, albumin appears to mitigate the toxicity of Cu(II)-bound Def but further studies are needed to understand why this is the case. More broadly, it would be important to determine whether the formation of such an albumin Cu(II) ternary complex could be a source of off-target toxicity of Def.

3. Conclusions

The observations of biological Cu(II) coordination by iron chelators (Def and Triapine) and the moderate cytotoxicity of the Cu(Def)(BSA) ternary complex and concentration-dependent Cu(II) scavenging by Def broadly suggest that extracellular Cu(II) chelation by iron chelators designed for therapeutic applications is an important interaction that needs to be further evaluated for the influence (positive or negative) it may have on the chelator's physiological effect. The boxed label for Def reports on the chelator's ability to lower Cu(II) and also Zn(II) serum levels with uncertain effects. It is important to note that the decreases of these metals induced by Def are comparable to what is observed for iron-overload treatment with the iron chelator deferoxamine.[33]

In addition, Cu(II) complexation by Def reveals a synergy of cytotoxicity that is worth exploring in future drug design. While the Cu(Def)(py) complex lacks cancer cell selectivity and ready solubility in water, future compound modifications can be done to optimize the cytotoxic potency even more while tuning the specificity for cancer cells.

Experimental Section

Materials

All aqueous solutions were prepared with autoclaved (121 °C and 18 PSI) high-quality nanopure water (18.2 MΩ cm resistivity, Pure-Lab Ultra Analytic water purification system). Acetonitrile (ACN), α-Cyano-4-hydroxycinnamic acid, dimethylformamide (DMF), Erastin, ethyl acetate, hexane, methanol, pyridine, salicylaldehyde, salicylamide, sodium dodecyl sulfate (SDS), thionyl chloride ($SOCl_2$),

pyridine, xylenes, N,N-dimethyl-p-phenylenediamine, and human ceruloplasmin were obtained from Millipore Sigma. Ferrostatin-1, Q-VD-OPh, and cisplatin (98%) were purchased from MedChem Express. Dimethyl sulfoxide (DMSO) and copper chloride ($CuCl_2$) in solid form and also as a 1 M aqueous solution (for affinity binding studies) were obtained from Fisher Scientific. A copper atomic absorption standard solution (1000 ppm) from Supelco was used for all Cu quantitative colorimetric assays. Corning™ Costar™ 96-Well, Cell Culture-Treated, U-Shaped-Bottom Microplate and Ceruloplasmin Colorimetric Activity Kit (#EIACPLC) were also obtained from Fisher Scientific. Bovine serum albumin was obtained from Cell Signaling Technology (#9998P). The protein was checked by SDS-PAGE to ensure the presence of only one protein band at ~66 kDa. Centrifugal filters (3 kDa MWCO) (centricons) were obtained from Pall Corporation. Bradford reagent for protein quantification was obtained from VWR. Potassium cyanide was obtained from Cambridge Isotope Laboratories. FerroZine (TM), Sodium Chloride, and Tris(hydroxymethyl)aminomethane were obtained from Acros Organics. A 10X PBS buffer solution was prepared by mixing 100 mM Na_2HPO_4, 18 mM KH_2PO_4, 1.37 M NaCl, and 27 mM KCl and adjusting the pH to 7.4. It was diluted 10-fold to yield 1X PBS (pH adjusted to 7.4 as needed) for several experiments in this manuscript. All other chemicals were of high purity and used as received. Wilmad quartz (CFQ) EPR tubes were obtained.

A549 human lung cancer cells (CCL-185™) and MRC-5 human lung fibroblasts (CCL-171™) were obtained from ATCC®. The cell lines were cultured in phenol red DMEM (Sigma, D6429) containing 1% glutamine, 4.5 g/mL of glucose, and sodium pyruvate. Media was supplemented with 10% FBS (HyClone) and 1% penicillin-streptomycin (Prepared from the solid obtained from Calbiochem, EMD Biosciences Inc. and prepared as follows: Streptomycin 11 mg/mL and Penicillin 7 mg/mL) at 37 °C in a humidified atmosphere of 5% (v/v) CO_2. Phenol Red-free DMEM (CellGro® REF 17–205-CV) was used during cytotoxicity studies. Corning™ Costar™ 96-Well, Cell Culture-Treated, Flat-Bottom Microplate was used to perform the cell viability assays. 3-(4,5-n-dimethylthiazole-2-yl)-2,5-diphenyl tetrazolium bromide (MTT) was purchased from Sigma-Aldrich. Dodecyl sulfate sodium salt (SDS, electrophoresis, 98% pure) was obtained from Acros Organics. Trypan blue solution (0.4%) was purchased from Sigma.

Instruments

All pH values were determined using a Thermo Scientific Orion Star A211 and an Orion 9157BNMD electrode or an Orion 8220BNWP, calibrated with standard buffer solutions at pH 4, 7, and 10. Absorbances were measured either with the Cary 300 UV-Vis spectrophotometer or a Thermo Scientific™ Spectrophotometer NanoDrop™ 2000/2000c. Multiwell plate absorbance was measured in a Tecan Infinite M200 PRO plate reader. Mass spectra were collected on a MALDI TOF/TOF AB SCIEX 4800 Analyzer and a Waters Micromass Q-TOF with electrospray ionization (ESI) at a capillary voltage of 3000 and sample cone voltage of 30. Theoretical MS were generated using the Isopro3 program. IR spectra were collected on a Nicolet IS 50 FT-IR Spectrometer. Continuous-wave (CW)-EPR spectra were recorded at the University of Arizona, EPR Facility on an X-band EPR spectrometer Elexsys E500 (Bruker). Cyclic voltammetry experiments were performed using a SP-240 potentiostat (Bio-logic Science Instrument). Cells were grown in a Revco Elite III RCO5000T-5-ABC incubator. Cell counting and culture viability monitoring were performed using a Nikon Eclipse TS-100 microscope.

Synthesis of 4-[(3Z,5E)-3,5-bis (6-Oxocyclohexa-2,4-Dien-1-Ylidene)-1,2,4-Triazolidin-1-yl] Benzoic Acid ($C_{21}H_{15}N_3O_4$), Deferasirox

2-(2-hydroxyphenyl)-4H-benzo[e][1,3]oxazin-4-one was synthesized as follows: Salicylic acid (10.0 g, 72.4 mmol, 1.00 eq.) and salicylamide (8.9 g, 65.0 mmol, 0.90 eq.) were dissolved in 45.0 mL of xylenes under Ar atmosphere. The mixture was stirred and pyridine (1.52 mL, 18.8 mmol, 0.26 eq.) was added. The reaction mixture was heated to reflux, and $SOCl_2$ (8.0 mL, 11.01 mmol, 1.52 eq) was added dropwise over 6 h. The mixture was left to react overnight. The next day, the reaction was cooled down to room temperature, and the precipitated solid was filtered and dried in a high vacuum. No significant impurities were observed by thin-layer chromatography (TLC) (80:20, Hexane: Ethyl acetate), and the following reaction was performed. Deferasirox was synthesized by reflux using the 2-(2-hydroxyphenyl)-4H-benzo[e][1,3]oxazin-4-one (14.9 g, 62.30 mmol, 1.00 eq.) previously synthesized and 4-hydrazine benzoic acid (7.16 g, 4.70 mmol, 0.65 eq.) in 140.0 mL of methanol. After a 2 h reaction, a pale-yellow solid was observed. The reaction was followed by TLC (80:20, Hexane: Ethyl acetate). After reaction completion, solid was obtained by rotovaporation, resuspended in 200 mL of acetone, and refluxed for 1.5 h. The hot mixture was filtered, and the solid was washed with small amounts of hot water. Solid was dried in high vacuum for 12 h. TLC showed a pure compound (Yield: 16.5 g, 71.3%). CHN elemental analysis was performed by Atlantic Microlabs (Norcross, GA): C, 67.69 (67.55); H, 4.26 (4.05); N, 11.05 (11.25). ^{1}H NMR (δ ppm d_6-DMSO, 500 MHz): 6.88 (d, 1H), 6.97–7.04 (m, 3H), 7.38 (m, 2H), 7.54 (d, 1H), 7.55 (d, 2H), 7.99 (d, 2H), 8.04 (d, 1H), 10.04 (s, OH), 10.80 (s, OH), 13.14 (broad, OH).

Synthesis of [Cu(Deferasirox)(Pyridine)] Pyridine 0.5 H_2O ($CuC_{26}H_{18}N_4O_4$ C_5H_5N 0.5 H_2O) (M. W. 602.11 g/mol)

117.5 mg (0.69 mmol, 1.7 eq) of $CuCl_2$ $2H_2O$ was dissolved in 5 mL of water and 148.6 mg (0.40 mmol, 1.0 eq) of deferasirox was dissolved in methanol following our previous protocol. The $CuCl_2$ solution was added dropwise to the ligand solution and a green precipitate formed. The precipitate was washed twice with methanol to remove unreacted ligand and it was collected by centrifugation at 4,000 rpm for 5 min. at room temperature. It was then washed three times by the same process with water to remove unreacted $CuCl_2$. The green solid was solubilized using pyridine producing a dark emerald green solution. After reacting for 2 h, water was added dropwise to precipitate the dark green product. The solvent was evaporated using a rotary evaporation followed by three water washes by centrifugation. The green solid was dried by lyophilization (yield 48%). CHN elemental analysis was performed by Atlantic Microlabs (Norcross, GA): C, 62.11; H, 3.77; N, 11.53. FT-IR (cm^{-1}): ν(C=O) 1699, 1599; ν(C–O) 1263,1236. UV-Vis (50:50 H_2O:Pyridine): λ_{max} 335 nm, $\varepsilon = 11{,}431.8\ M^{-1}cm^{-1}$. ESI-MS (positive): m/z 514.08, $\{H^+ + [Cu(Def)(py)]\}^+$; $\{H^+ + [CuC_{26}H_{18}N_4O_4]\}^+$. The EPR spectrum (frozen 50:50 H_2O:pyridine (v/v), 77 K) is typical for a mononuclear Cu(II) complex, characterized by a slightly rhombic g-tensor with ($g_\perp$, $g_{||} = 2.05$, 2.26) and near-axial hyperfine interaction (hfi) of the copper nucleus with ($A_\perp$, $A_{||}$ = ~0,471.0 MHz).

Cyclic Voltammogram Analysis of [Cu(Deferasirox)(pyridine)] and $Cu(py)_4^{2+}$

The reduction potentials of 2 mL of 7.11 mM Cu(Def)(py) and of 7 mM $Cu(py)_4^{2+}$ in 25% pyridine (v/v):75% 500 mM KCl (aq) (adjusted to pH = 7.4) were measured by cyclic voltammetry (CV). A stock 28.45 mM $Cu(py)_4^{2+}$ solution was prepared in situ by diluting $CuCl_2$ (aq) in pyridine.[14,15] A stock solution of 28.45 mM Cu(Def)(py)

solution was prepared in pyridine. These solutions were then diluted in the salt solution.The background solution was made by diluting pyridine to 25% with 75% 500 mM KCl (aq) (adjusted to pH = 7.4). Cyclic voltammograms were measured in a three-electrode cell consisting of a 2.0 mm diameter Platinum (Pt) working electrode, a Pt auxiliary electrode, and an Ag/AgCl reference electrode containing 0.1 M KCl in water. All samples were deaerated by passing a stream of Ar through them before measurements and then maintaining a blanket of Ar over them during measurements. All measurements were performed with 4 scans at a scan rate of 50 mV/s. The final results are reported relative to the normal hydrogen electrode (NHE).

EPR Analysis of [Cu(Deferasirox)(pyridine)]

A 5 mM [Cu(Deferasirox)(py)] solution (1 mL) was prepared in pyridine. The solution was transferred to EPR tubes and frozen in liquid N_2 before EPR analysis. The EPR experiments were performed using the following conditions: microwave frequency, 9.463 GHz; microwave power, 200 mW; magnetic field modulation amplitude, 0.2 mT for Cu(II) (S = 1/2) detection, temperature: 77 K.

Quantifying of Cu Concentration in Protein and Protein-Free Samples by a Modified Ferrozine Assay

All glassware was acid-washed to eliminate trace metal contamination. A ferrozine ligand solution is prepared by dissolving 0.0102 g ferrozine and 0.2 g hydroxylamine hydrochloride in 10 mL of 500 mM KH_2PO_4 buffer (pH = 7.5). This solution must be prepared fresh each day before performing the assay. For samples containing protein, the sample is digested by mixing equal volume sample with 30% trichloroacetic acid (TCA) (w/v) aqueous solution. The sample was boiled for 5 min and left resting for 1 h. It was then sonicated for five minutes. The supernatant was collected and the pH was adjusted to 7.5 with a minimum of 10 M NaOH. For protein-free samples, the digestion step could be skipped and no pH adjustment of final solutions was needed. A background solution containing 50:50 buffer/TCA ratio (pH = 7.5) was used for preparation of the final set of solutions for protein containing samples. A calibration curve was made using a Cu standard solution of 1000 ppm (15.74 mM) and diluted to the concentration range 10 μM–200 μM in 10 mM HCl (aq). The final solutions of the standards contained the same volume of the solution background of the samples to minimize any background matrix effects. In a 96-well microplate (transparent flat bottom), equal parts ferrozine solution were mixed with the Cu standards or samples (n = 4). The hydroxylamine in the ferrozine solution reduced Cu(II) to Cu(I), allowing for ferrozine to coordinate the Cu(I) forming a 1:2 Cu(I):ferrozine complex[34] (ε = 3892 $M^{-1}cm^{-1}$). These samples were scanned by nanodrop and corrected at 750 nm (as a measure of light scattering). The data for the standards were fitted to a linear equation and the Cu concentration is determined from the absorbance using this equation and correcting for any dilution.

Determination of the Formation Constant of Cu(Def)(py)

A spectrophotometric metal ligand complexation experiment was performed at pH 7.4 and I = 0.1 M. A commercial source of 1 M $CuCl_2$ was used for this experiment to create 20 mM $Cu(py)_4$ in situ by dilution in pyridine.[14,15] A stock solution of 20 mM deferasirox was prepared in DMF. To separate 2 mL solutions of 50 μM $Cu(py)_4$ were added varying concentrations of deferasirox (25–350 μM) in a background that contained 50% pyridine (v/v) in 20 mM HEPES buffer (0.1 M NaCl, pH 7.4). These solutions all contained a constant 2.5% DMF (v/v).The solutions were equilibrated for 24 h at RT and then their absorbances were scanned by a UV-Vis spectrophotometer in the wavelength range of 250–800 nm. A binding curve for the formation of Cu(Def)(py) was generated from the increase in absorbance at 346 nm in response to the increase in initial Def concentration after processing the amount of Def and Cu(Def)(py) at equilibrium.

Solution Stability Study of Cu(Def)(py)

A fresh stock solution of 2 mM Cu(Def)(py) was prepared in pyridine. It was diluted to 40 μM with water (pH = 9.00) and with 5 mM NH_4HCO_3 buffer (pH = 7.4). The background of these solutions contained 2% pyridine (v/v). The solutions were monitored by UV Vis spectroscopy for three days.

Study of the Cu(II) Scavenging Capability of Deferasirox from Serum Albumin

A 200 μM stock solution of 40 mg (0.06 mmol) of BSA was dissolved in 3 mL of 20 mM HEPES buffer (0.1 M NaCl, pH 7.4) and washed three times in the buffer using a 3 kDa centricon (4,400 rpm for 20 min). An in situ 5 mM $[Cu(Tris)_4]^{2+}$ was prepared following a literature protocol[35] by diluting 1.515 mL of 165 mM $CuCl_2$ (aq) (quantified by the ferrozine assay) in 0.1 M Tris buffer (0.1 M NaCl, pH 7.4) to a final 50 mL volume. The solution was equilibrated overnight and the pH was confirmed to stay at 7.4. A 60 μM Cu(II)-bound BSA solution was prepared by reacting the BSA stock solution with the $[Cu(Tris)_4]^{2+}$ stock solution at a 1:1 stoichiometric ratio to avoid Cu(II) binding beyond the ATCUN site. The reaction mixture was left to equilibrate for 2 h. It was then washed twice with the 3 kDa centricon in the Tris buffer and then three times in the HEPES buffer. The switch in buffer was to switch to a low Cu(II) binding buffer. The concentration of bound Cu(II) and of protein was determined by the ferrozine and Bradford assays, respectively, and they were found to be 1:1 Cu:protein.

Cu(II)-bound BSA was then reacted with Def at a 1:1 protein:chelator ratio. Due to the poor water solubility of Def, it was dissolved in DMSO first and then diluted into the HEPES buffer. The reaction mixture contained 0.3% DMSO, a percentage that does not harm the protein integrity. Initially the reaction was monitored by UV Vis every 5 min for 60 mi and then every hour for up to 12 h but the reaction went to completion even before the initial 5 min. The spectrum features an absorbance maximum at 340 nm with an extinction coefficient of 12,010 $M^{-1}cm^{-1}$ characteristic of a LMCT. To validate this result, a titration was set up in separate eppies by mixing 60 μM Cu(II)-bound BSA solution with 0.1 mole equivalents of Def. The growth of the LMCT at 338 nm was plotted versus the concentration of Def in molarity and the line of best fit ($y = 0.01201x + 0.04106$) yielded a comparable extinction coefficient. A control reaction was performed by preparing a 60 μM Cu(II) solution by direct dilution of the $Cu(Tris)_4$ stock solution into the buffer solution and reacting it with equimolar Def.

The reaction of Cu(II)-bound BSA with Def was also evaluated by electron paramagnetic resonance under two conditions. One reaction was prepared as previously described by mixing the protein with Def at 60 μM equimolar amounts. The reaction was scanned by UV-Vis to confirm full conversion to the final product as verified by the extinction coefficient at 338 nm. This solution was then washed with the HEPES buffer and then concentrated to 1.63 mM using the 3 kDa centricon. It was then mixed with glycerol to a 50:50 mixture to yield 815 μM. In a separate reaction, Cu(II)-bound BSA was mixed with Def at 500 μM equimolar amounts. This reaction immediately produced a green precipitate and the UV-Vis spectrum revealed no presence of the LMCT at 338 nm. This solution was washed with the HEPES buffer and then concentrated to 1 mM using the 3 kDa centricon. It was then mixed with glycerol to a 50:50 mixture to yield 500 μM. A 500 μM Cu(II)-bound BSA sample was also prepared for EPR measurement. The samples were pipetted in EPR tubes (O.D. 4 mm, L 250 mm), ensuring a

sample height of 20–25 mm (about 140–170 μL). Each sample was then frozen in liquid N_2, and then carefully mailed to be measured by EPR. Experimental conditions: microwave frequency, 9.443 GHz; microwave power, 20–30 db; magnetic field modulation amplitude, 0.5 mT; temperature, 77 K.

Study of Deferasirox Inhibition of Ceruloplasmin Activity

Ceruloplasmin enzymatic activity was determined with a colorimetric assay kit, using N, N-dimethyl-p-phenylenediamine as substrate and commercially bought human ceruloplasmin. 2X assay buffer was diluted to 1X for assay purposes as established in the kit protocol. A 2000 mU/mL ceruloplasmin stock solution was prepared in 1X assay buffer and diluted to assay concentrations (31.25–1000 mU/mL). These solutions were used to assess the linearity of enzyme activity via a standard curve. A 2 mM Cu(deferasirox)(pyridine) solution was prepared in pyridine and a 4 mM deferasirox solution was prepared in DMF. Potassium cyanide was dissolved in water to 400 μM and used as a negative control.[23] Ceruloplasmin (1000 mU/mL) samples were reacted with deferasirox (100 μM), Cu(deferasirox)(pyridine) (100 μM), or potassium cyanide (10 μM) in a total volume of 100 μL. Samples containing Cu-(deferasirox)(pyridine) were prepared in 2.5% pyridine and 97.5% 1X assay buffer. All other reactions were prepared in solutions with a constant 2.5% DMF and 97.5% 1X assay buffer. Samples without ceruloplasmin, substrate, or experimental compounds were substituted with an equivalent volume of 1X assay buffer. A control sample with 2.5% pyridine and 97.5% 1X buffer was prepared. All samples ($n=4$) were equilibrated for 1 h at RT. Subsequently, each sample was added 25 μL of substrate (unless noted otherwise) and equilibrated for 1 h at 30 °C in a 96-well plate. The absorbance of each sample was immediately measured at 560 nm using the Tecan plate reader.

National Cancer Institute Cancer Cell Line (NCI-60) Screen of Deferasirox and Cu(Def)(py)

Details of the methodology for NCI-60 cell line screening are described at https://dtp.cancer.gov/discovery_development/nci-60/announcement.htm. The cells, grown in supplemented RPMI-1640 medium, were seeded in 96 well plates at an appropriate density and incubated for 24 h. The Def and Cu(Def)(py) were dissolved in DMSO and incubated with cells at a single dose of 10.0 μM, followed by a 400-fold dilution in cell medium, for 72 h. The cell viability was measured by the Cell Titer-Glo assay and the % cell growth relative to the nontreated control was reported.

Cell Culturing

Thawed stocks of A549 and MRC-5 cells were washed with 1X PBS and resuspended in phenol red DMEM media (supplemented with 10% FBS and 1% penicillin-streptomycin) and then seeded in a 100 mm×20 mm (complete, O.D. x H) petri dish and grown in a 5% (v/v) CO_2 humidified atmosphere at 37 °C. At least three passages were performed to ensure the integrity of the cells.

Cell Viability Studies to Determine the Antiproliferative/Cytotoxic Property of Cu(Def)(py)

Cultured cells were collected, thoroughly washed with 1X PBS, and then resuspended in phenol red-free DMEM (supplemented with 10% FBS, 1% penicillin-streptomycin, and 4 mM L-glutamine). These cell viability studies were performed using A549 cells at a 1.0×10^5 cells/mL density and MRC5 cells at a 2.0×10^5 cells/mL density, respectively. A volume of 50 μL of cells was seeded into 96-well plates. Cells were incubated for 24 h. A stock solution of Cu(Def)(py) was prepared fresh in pyridine at a concentration of 20 mM and a fresh solution of Cu(Def)(BSA) was made at 200 μM in 20 mM HEPES buffer (100 mM NaCl, pH = 7.4). The Cu(Def)(py) stock solution was diluted in 1X PBS to a concentration range of 4 nM to 80 μM while keeping the background concentration of 0.70% pyridine (v/v). The same concentration range was prepared for Cu(Def)(BSA) in the HEPES buffer. The cells were treated with 50 μL of the Cu(II) compound solutions. Control wells in the plates consisted of one lane of cells treated with equal volume of the HEPES buffer or 1X PBS with 0.7% pyridine (v/v). These lanes serve as the measure of 100% viable cells in the media. Another control lane consisted of 50 μL media with no cells mixed with equal volume of HEPES buffer or 1X PBS with 0.7% pyridine (v/v). This lane serves as the measure of 0% viable cells in the media. Cells were incubated for 68 h. At this time, 50 μL MTT solution (1.5 mg/mL in 1X PBS, pH 7.4) was added with mixing. After 4 h, 25 μL of 20% (w/v) SDS (prepared in 0.1 M Tris buffer at pH 11) was added to solubilize the purple formazan product crystals and left overnight in the incubator. The plates were read at the wavelength of 570 nm (absorbance of the formazan product at $pH > 10.0$)[36] and 800 nm (as a correction for light scattering) using a Tecan plate reader. The absorbance of all wells was compared to the absorbance of the untreated cells with the MTT set as the 100% viable cell standard and the absorbance of the no cell control set as the 0% viable cell standard. Nonlinear regression in Origin 8.5 was utilized to fit the growth curves using the pharmacology single-phase and biphase dose-response equation as deemed appropriate to determine the half-maximal inhibitory concentration (IC_{50}) and the corresponding standard deviation. All samples were tested six times. This same cell viability experiment approach was used in subsequent cell experiments.

Evaluating the capacity of Deferasirox and Cu(Def)(py) to induce apoptosis and ferroptosis. Ferroptosis and apoptosis induction by Def and Cu(Def)(py) were investigated in A549 cells using the ferroptosis inhibitor ferrostatin-1 (Fer-1) and caspase-dependent apoptosis inhibitor Q-VD-OPh in cell viability studies. Cultured cells were collected, thoroughly washed with 1X PBS, and then resuspended in phenol red-free DMEM (supplemented with 10% FBS, 1% penicillin-streptomycin, and 4 mM L-glutamine) at a 1.0×10^5 cells/mL concentration. A volume of 50 μL of cells was seeded into six lanes of 96-well plates. One lane was filled with 50 μL of media. The cells were incubated for 24 h. Stock solutions of Def, Fer-1, Q-VD-OPh, erastin (a ferroptosis inducer), and cisplatin (a caspase-dependent apoptosis inducer) were prepared in DMF. These solutions were diluted with 1X PBS to a final 1% DMF (v/v). Some of the cells were treated with 25 μL of 40 μM of Fer-1 or with 25 μL of 40 μM of Q-VD-OPh for 2 h. After the 2 h, cells with and without Fer-1 were treated with 25 μL of 40 μM of erastin and with and without Q-VD-OPh were treated with 25 μL of 40 μM of cisplatin. Cell with and without the inhibitors were treated with 25 μL of 200 μM of Def or with 25 μL of 20 μM of Cu(Def)(py). The concentrations of compounds were selected to induce ~80% inhibition of cell proliferation. Untreated cells and no cell wells were mixed with equal volume of 1X PBS with 1% DMF (v/v). All final solutions contained 0.5% (v/v) DMF and 100 μL volume. The lane with no compound treatment serves as the measure of 100% viable cells in the media and the lane with no cells serves as the measure of 0% viable cells. Cells were incubated for 68 h and the MTT assay was performed as described for protein-free solutions. All samples were tested six times for the biological triplicates. A student t-Test was performed to compare changes in cell viability in the presence and absence of co-treatment with the cell death inhibitors.

Acknowledgements

A.D.T. and his team thank the NIH 5SC1CA190504 grant, the NIH 1R21CA240997-01 A1 grant (which also funded L.F.-V. and J.A.B.-R.), and the American Cancer Discovery Boost DBG-23-1156894-01-ET

(which also funded S.L.S.-C.) grant for their financial support. L.F.-V. extends her special thanks to Proyecto Título V UPR-RCM PO31S200104 for their current support, additionally to the University of Puerto Rico Río Piedras PBMA fellowship and the University of Puerto Rico Río Piedras FIPI grant (which also funded A.M.O.R.) during her PhD studies. A.M.O.R. wishes to acknowledge the NIH G-RISE 1T32 GM152384-01 for their current support, the NIH RISE 5R25 GM061151 (which also funded L.A.L.-C., J.A.V.A., A.V.-F., and J.A.B.-R.), and the Center for Neuroplasticity at the University of Puerto Rico COBRE II Grant (5P30 GM149367) for their financial assistance. L.A.L.-C. wishes to acknowledge the support of the NIH U-RISE 1T34 GM153667-01 grant. J.A.B.-R. thanks the support of the NSF STC Bioxfel 1231306 grant. M.V.P.O. thanks the MSEIP P120 A210035 grant (which also supported A.M.O.R.). M.R. and V.B.E. acknowledge the financial support from NSF REU grants (2349168 and REU CHE 1757365, respectively), which aided their participation in this research experience. The authors acknowledge Mildred Rivera-Isaac (UPR-MCC) for her help with the ESI-MS experiments and Alejandro Burgos-Suazo for facilitating use of the Thermo Fisher™ Nicolet™ IS 50 FT-IR Spectrometer. We acknowledge Dr. Eduardo Nicolau and Nerika G. Hernandez for access and technical support in our cyclic voltammetry experiments. The graphical abstract was prepared using Biorender.

Conflict of Interests

The authors declare no conflict of interest.

Data Availability Statement

The data that support the findings of this study are available in the supplementary material of this article.

Keywords: Cancer · Copper · Deferasirox · Iron chelator · Toxicity

[1] S. Tury, F. Assayag, F. Bonin, S. Chateau-Joubert, J.-L. Servely, S. Vacher, V. Becette, M. Caly, A. Rapinat, D. Gentien, P. de la Grange, A. Schnitzler, F. Lallemand, E. Marangoni, I. Bièche, C. Callens, *J. Pathol.* **2018**, *246*(1), 103–114.
[2] W.-Y. Hsu, L.-T. Wang, P.-C. Lin, Y.-M. Liao, S.-H. Hsu, S.-S. Chiou, *Antioxidants* **2024**, *13*(4), 424.
[3] S. A. Loza-Rosas, A. M. Vazquez-Salgado, K. I. Rivero, L. J. Negron, Y. Delgado, J. A. Benjamin-Rivera, A. L. Vazquez-Maldonado, T. B. Parks, C. Munet-Colon, A. D. Tinoco, *Inorg. Chem.* **2017**, *56*(14), 7788–7802.
[4] K. Gaur, S. C. Perez Otero, J. A. Benjamin-Rivera, I. Rodriguez, S. A. Loza-Rosas, A. M. Vazquez Salgado, E. A. Akam, L. Hernandez-Matias, R. K. Sharma, N. Alicea, M. Kowaleff, A. V. Washington, A. V. Astashkin, E. Tomat, A. D. Tinoco, *JACS Au* **2021**, *1*(6), 865–878.
[5] C. N. Kontoghiorghe, G. J. Kontoghiorghes, *Drug Des. Dev. Ther.* **2016**, *10*, 465–481.
[6] J. B. Porter, A. T. Taher, M. D. Cappellini, E. P. Vichinsky, *Hemoglobin* **2008**, *32*(6), 601–607.
[7] J. D. Díaz-García, A. Gallegos-Villalobos, L. Gonzalez-Espinoza, M. D. Sanchez-Niño, J. Villarrubia, A. Ortiz, *Nat. Rev. Nephrol.* **2014**, *10*(10), 574–586.
[8] E. M. Gottwald, C. D. Schuh, P. Drücker, D. Haenni, A. Pearson, S. Ghazi, M. Bugarski, M. Polesel, M. Duss, E. M. Landau, A. Kaech, U. Ziegler, A. K. M. Lundby, C. Lundby, P. S. Dittrich, A. M. Hall, *Sci. Rep.* **2020**, *10*(1), 1577.
[9] S. Steinhauser, U. Heinz, M. Bartholomä, T. Weyhermüller, H. Nick, K. Hegetschweiler, *Eur. J. Inorg. Chem.* **2004**, *2004*(21), 4177–4192.
[10] I. Rodríguez, L. Fernández-Vega, A. N. Maser-Figueroa, B. Sang, P. González-Pagán, A. D. Tinoco, *Antibiotics* **2022**, *11*(2), 158.
[11] U. Heinz, K. Hegetschweiler, P. Acklin, B. Faller, R. Lattmann, H. P. Schnebli, *Angew. Chem. Int. Ed.* **1999**, *38*(17), 2568–2570.
[12] T. Zandvakili, S. Jamil Fatemi, S. Yousef Ebrahimipour, H. Ebrahimnejad, J. Castro, M. Dusek, V. Eigner, *J. Mol. Struct.* **2022**, *1249*, 131525.
[13] J. Peisach, W. E. Blumberg, *Arch. Biochem. Biophys.* **1974**, *165*(2), 691–708.
[14] D. L. Leussing, R. C. Hansen, *J. Am. Chem. Soc.* **1957**, *79*(16), 4270–4273.
[15] M. S. Sun, D. G. Brewer, *Can. J. Chem.* **1967**, *45*(22), 2729–2739.
[16] P. Zelenay, L. M. Rice-Jackson, A. Wieckowski, *Langmuir* **1990**, *6*(5), 974–979.
[17] A. J. Lucio, S. K. Shaw, *J. Phys. Chem. C* **2015**, *119*(22), 12523–12530.
[18] Z. Chen, R. Jiang, M. Chen, J. Zheng, M. Chen, N. Braidy, S. Liu, G. Liu, Z. Maimaitiming, T. Shen, J. L. Dunaief, C. D. Vulpe, G. J. Anderson, H. Chen, *Sci. Rep.* **2019**, *9*(1), 9437.
[19] M. C. Linder, *Metallomics* **2016**, *8*(9), 887–905.
[20] I. Bento, C. Peixoto, V. N. Zaitsev, P. F. Lindley, *Acta Crystallogr. D Biol. Crystallogr.* **2007**, *63(Pt 2)*, 240–248.
[21] T. Brody, *Nutritional Biochemistry* Elsevier Inc. Academic Press, San Diego CA, **1999**■■Dear Author please add pagenumbers or eLocator■■.
[22] D. E. Heppner, C. H. Kjaergaard, E. I. Solomon, *J. Am. Chem. Soc.* **2014**, *136*(51), 17788–17801.
[23] M. V. Chidambaram, G. Barnes, E. Frieden, *J. Inorg. Biochem.* **1984**, *22*(4), 231–240.
[24] G. J. van der Vusse, *Drug Metab. Pharmacokinet.* **2009**, *24*(4), 300–307.
[25] M. Moriya, Y. H. Ho, A. Grana, L. Nguyen, A. Alvarez, R. Jamil, M. L. Ackland, A. Michalczyk, P. Hamer, D. Ramos, S. Kim, J. F. Mercer, M. C. Linder, *Am. J. Physiol. Cell Physiol.* **2008**, *295*(3), C708–721.
[26] K. Bossak-Ahmad, T. Frączyk, W. Bal, S. C. Drew, *ChemBioChem* **2020**, *21*(3), 331–334.
[27] M. Lefèvre, K. P. Malikidogo, C. Esmieu, C. Hureau, *Molecules* **2022**, *27*(22)■■Dear Author, please add page number in Refs. [27].■■.
[28] M. Schaier, E. Falcone, T. Prstek, B. Vileno, S. Hager, B. K. Keppler, P. Heffeter, G. Koellensperger, P. Faller, C. R. Kowol, *Metallomics* **2023**, *15*(8)■■Dear Author please add page number in Refs. [28].■■.
[29] R. A. Finch, M. Liu, S. P. Grill, W. C. Rose, R. Loomis, K. M. Vasquez, Y. Cheng, A. C. Sartorelli, *Biochem. Pharmacol.* **2000**, *59*(8), 983–991.
[30] K. Ishimaru, M. Ikeda, H. D. Miyamoto, S. Furusawa, K. Abe, M. Watanabe, T. Kanamura, S. Fujita, R. Nishimura, T. Toyohara, S. Matsushima, T. Koumura, K. i Yamada, H. Imai, H. Tsutsui, T. Ide, *J. Am. Heart Assoc.* **2024**, *13*(1), e031219.
[31] S. B. Jadhav, C. Sandoval-Acuña, Y. Pacior, K. Klanicova, K. Blazkova, R. Sedlacek, J. Stursa, L. Werner, J. Truksa, *bioRxiv* **2024**, ■■Dear Author please provide complete details in Refs. [31],■■ 2024.2001.2017.575692.
[32] V. A. Timoshnikov, L. A. Kichigina, O. Y. Selyutina, N. E. Polyakov, G. J. Kontoghiorghes, *Molecules* **2021**, *26*(16), 5064.
[33] M. D. Cappellini, A. Cohen, A. Piga, M. Bejaoui, S. Perrotta, L. Agaoglu, Y. Aydinok, A. Kattamis, Y. Kilinc, J. Porter, M. Capra, R. Galanello, S. Fattoum, G. Drelichman, C. Magnano, M. Verissimo, M. Athanassiou-Metaxa, P. Giardina, A. Kourakli-Symeonidis, G. Janka-Schaub, T. Coates, C. Vermylen, N. Olivieri, I. Thuret, H. Opitz, C. Ressayre-Djaffer, P. Marks, D. Alberti, *Blood* **2006**, *107*(9), 3455–3462.
[34] M. Körner, P. A. Tregloan, R. V. Eldik, *Dalton Trans.* **2003**,■■Dear Author, please add volume number in Refs. [34].■■ *(13)*, 2710–2717.
[35] A. E. Martell, R. M. Smith, *Critical Stability Constants* Springer, Boston, **1982**■■Dear Author please add pagenumbers or eLocator■■.
[36] J. A. Plumb, R. Milroy, S. B. Kaye, *Cancer Res.* **1989**, *49*(16), 4435–4440.

Manuscript received: November 19, 2024
Revised manuscript received: December 17, 2024
Version of record online: ■■, ■■

RESEARCH ARTICLE

Off-target effects from clinical use of deferasirox, an oral iron chelator drug, have prompted the study of its high affinity Cu(II) complexation and physiologically relevant speciation. Cu(II) coordination in small molecule form and by ternary complexation with the albumin ATCUN site provide insight into chelation toxicity and the cytotoxic synergism between the metal and chelator for potential anticancer drug development.

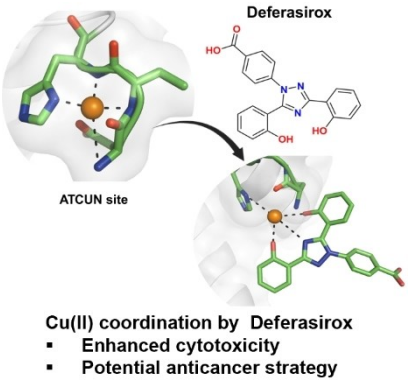

A. M. Orta Rivera, L. A. Landrau Correa, S. L. Schiavone-Chamorro, M. Rankins, M. V. Pérez Otero, J. A. Benjamín-Rivera, J. A. Vega Aponte, V. B. Ebenki, A. I. Vargas Figueroa, A. V. Astashkin, L. Fernández-Vega, A. D. Tinoco**

SPACE RESERVED FOR IMAGE AND LINK

Share your work on X! ChemMedChem promotes selected articles on X (formerly known as Twitter). Each article post contains the title, name of the corresponding author, a link to the article, selected handles and hashtags, and the ToC picture. If you, your team, or your institution have an X account, please include its handle @username below. We recommend sharing and interacting with these posts through your personal and/or institutional accounts to help increase awareness of your work! Please follow us @Chem_Europe.

ORCID (Open Researcher and Contributor ID)

Please check that the ORCID identifiers listed below are correct. We encourage all authors to provide an ORCID identifier for each coauthor. ORCID is a registry that provides researchers with a unique digital identifier. Some funding agencies recommend or even require the inclusion of ORCID IDs in all published articles, and authors should consult their funding agency guidelines for details. Registration is easy and free; for further information, see http://orcid.org/.

Aixa M. Orta Rivera
Luis A. Landrau Correa
Selene L. Schiavone-Chamorro
Moriana Rankins
Mariela V. Pérez Otero
Josué A. Benjamín-Rivera
José A. Vega Aponte
Valerie B. Ebenki
Adriana I. Vargas Figueroa
Andrei V. Astashkin
Lauren Fernández-Vega
Arthur D. Tinoco http://orcid.org/0000-0003-2825-5235

Elucidating the high affinity copper(II) complexation by the iron chelator deferasirox provides therapeutic and toxicity insight

Aixa M. Orta Rivera,[a] Luis A. Landrau Correa,[b] Selene L. Schiavone-Chamorro,[b] Moriana Rankins,[a] Mariela V. Pérez Otero,[b] Josué A. Benjamín-Rivera,[a] José A. Vega Aponte,[a] Valerie B. Ebenki,[a] Adriana I. Vargas Figueroa,[a] Andrei V. Astashkin,[c] Lauren Fernández-Vega,[d]* and Arthur D. Tinoco[a]*

[a] A.M. Orta Rivera, M. Rankins, J.A. Benjamín-Rivera, J.A. Vega Aponte, V.B. Ebenki, A.I. Vargas Figueroa, Prof. Arthur D. Tinoco
Department of Chemistry
University of Puerto Rico, Río Piedras Campus
Río Piedras, Puerto Rico 00925-2537, United States
E-mail: arthur.tinoco@upr.edu
[b] L.A. Landrau Correa, S.L. Schiavone-Chamorro, M.V. Pérez Otero
Department of Biology
University of Puerto Rico, Río Piedras Campus
Río Piedras, Puerto Rico 00925-2537, United States
[c] Dr. A.V. Astashkin
Department of Chemistry and Biochemistry
The University of Arizona
Tucson, AZ 85721-0041, United States
[d] Prof. L. Fernández-Vega
Division of Science, Technology, and Environment
University Ana G. Méndez-Cupey Campus
1399 Av. Ana G. Méndez, San Juan, PR 00926, United States
E-mail: lafernandez@uagm.edu

Supporting Information

Table of Contents

1. Supporting Figures

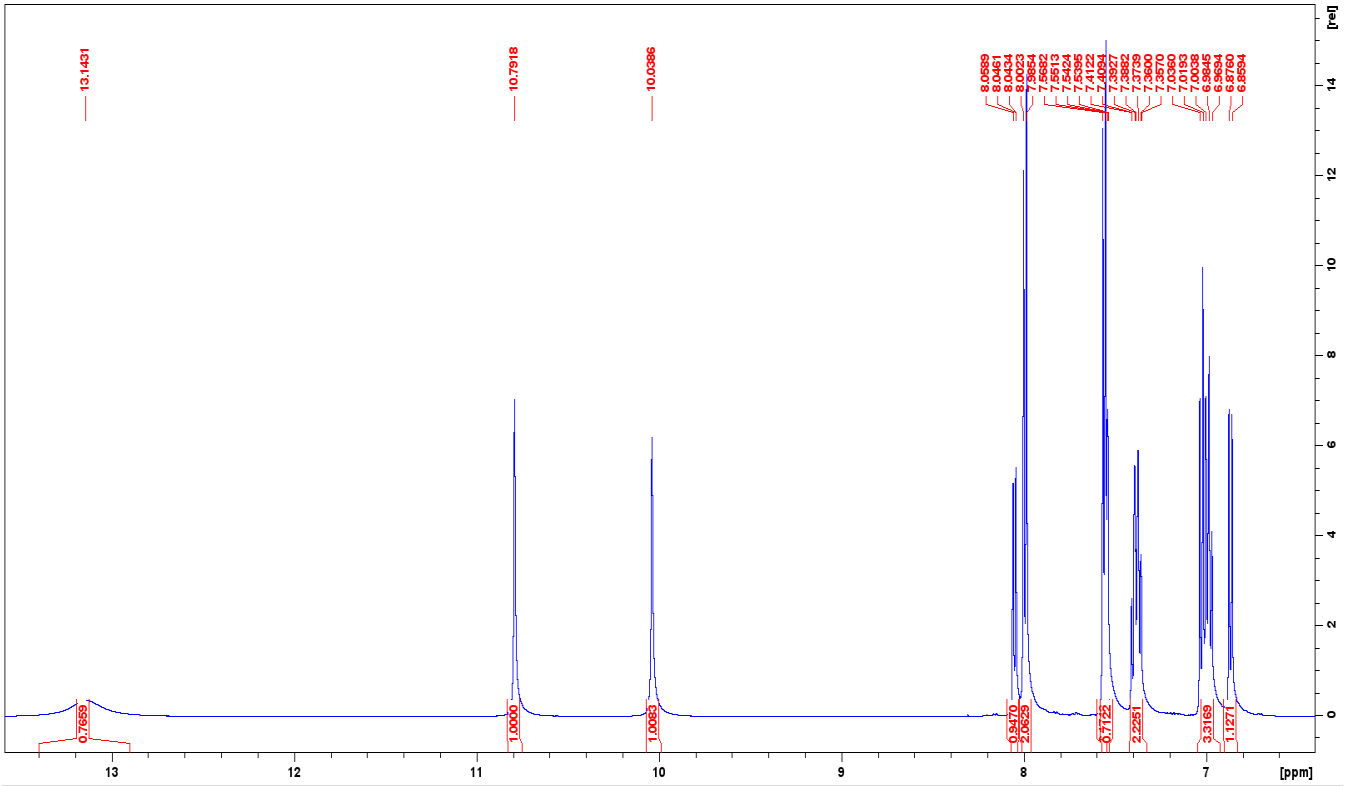

Figure S1. ^{1}H NMR spectrum of Deferasirox [Conditions: 500 MHz, number of scans 64, solvent DMSO-d6].

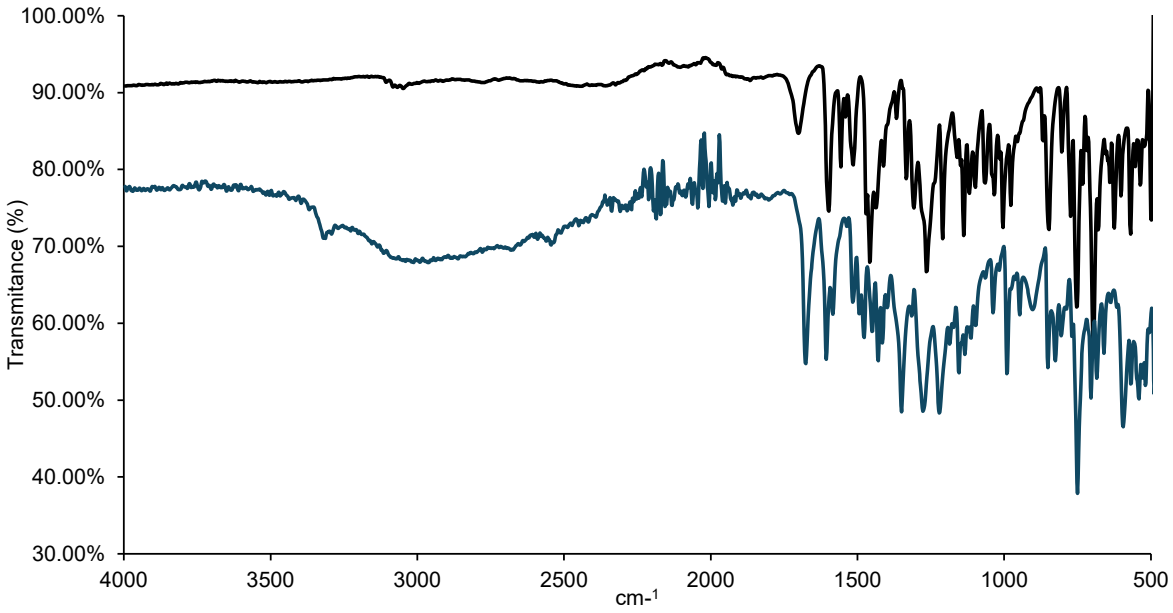

Figure S2. FTIR spectra of Deferasirox (blue line) and [Cu(Def)(py)] complex (black line).

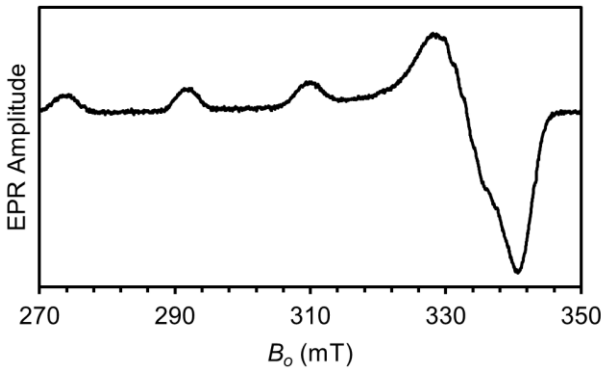

Figure S3. EPR spectrum of Cu(Def)(py) in frozen pyridine/water 50:50 (v/v) solution. Experimental conditions: microwave frequency, 9.463 GHz; microwave power, 200 mW; magnetic field modulation amplitude, 0.2 mT; temperature, 77 K.

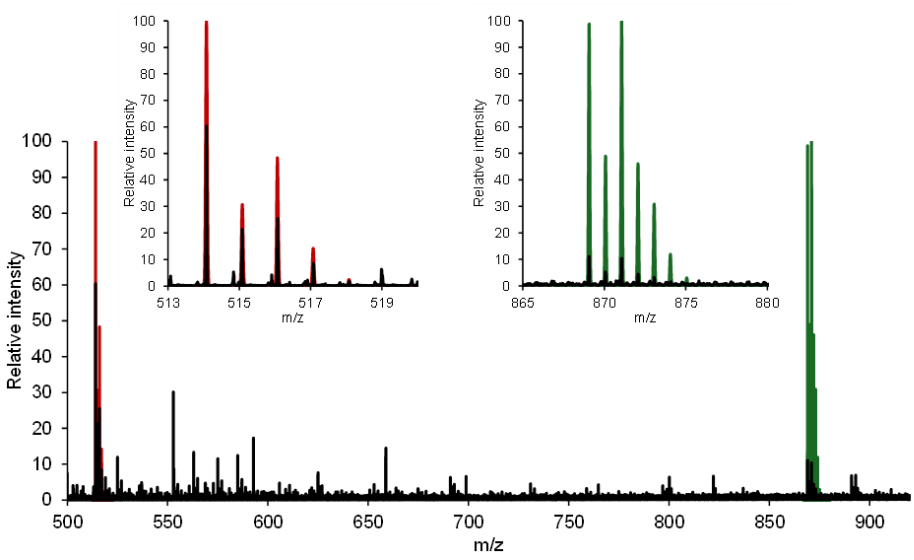

Figure S4. The ESI mass spectrum for the Cu(Def)(py) sample. Two main Cu species were identified: mononuclear Cu(Def)(py) ($C_{26}H_{18}N_4O_4Cu$ + H^+= 514.08 m/z) and dinuclear $[Cu(Def)]_2$ ($C_{42}H_{26}N_6O_8Cu_2$ + H^+= 871.06 m/z). The theoretical spectra are overlaid over the experimental in red (Cu(Def)(py)) and green ($[Cu(Def)]_2$) colors.

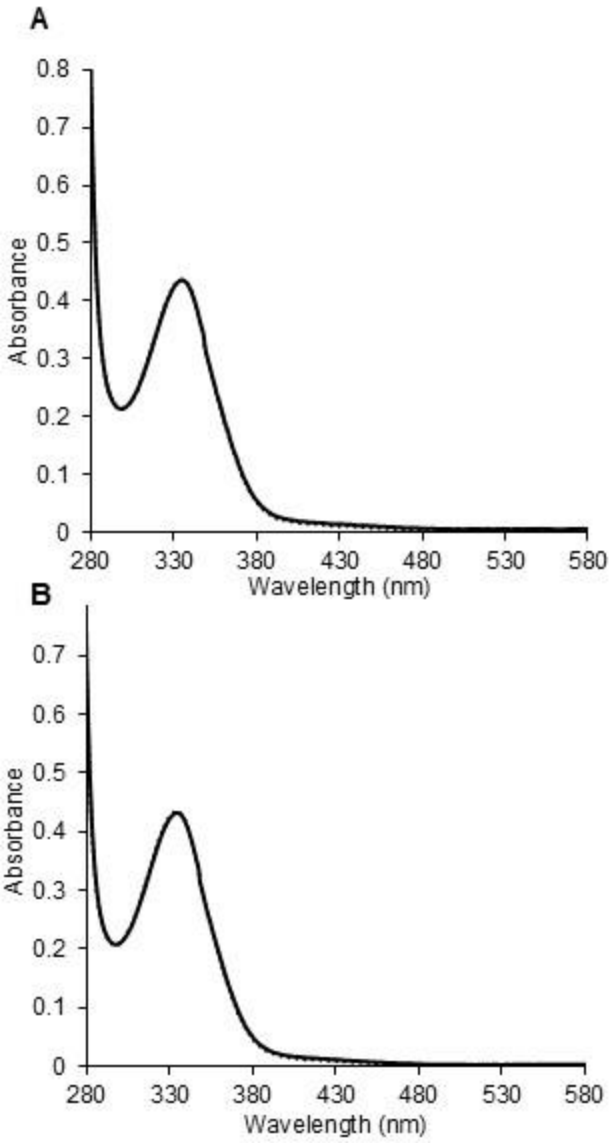

Figure S5. Stability studies of Cu(Def)(py) in aqueous solutions over 3 days. (A) The stability of 40 μM Cu(Def)(py) in 2% pyridine (v/v) in water. (B) The stability of 40 μM Cu(Def)(py) in 2% pyridine (v/v) in 5 mM NH_4HCO_3 (aq). The black lines are the spectra at day 1, and the dashed lines are the spectra at day 3.

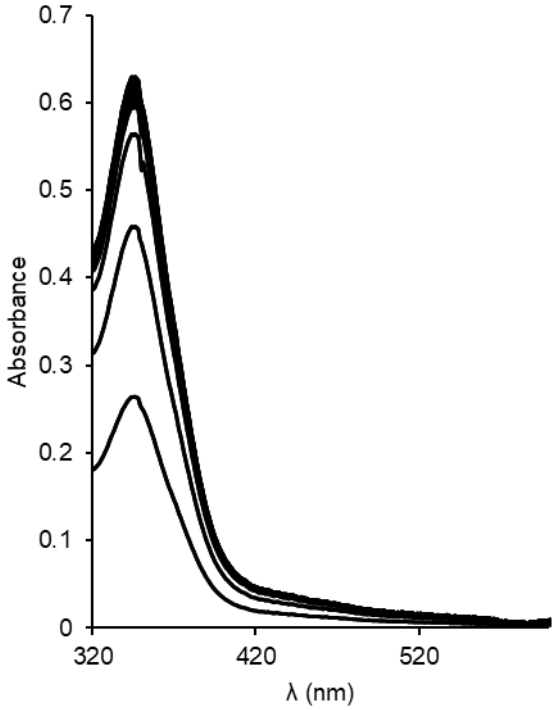

Figure S6. The growth in the LMCT band for Cu(Def)(py) from the reaction of 50 μM $Cu(py)_4$ with increasing mole equivalents of Def monitored by UV-Vis spectroscopy. The increments were from 0.5 equivalents up to 7.5 equivalents.

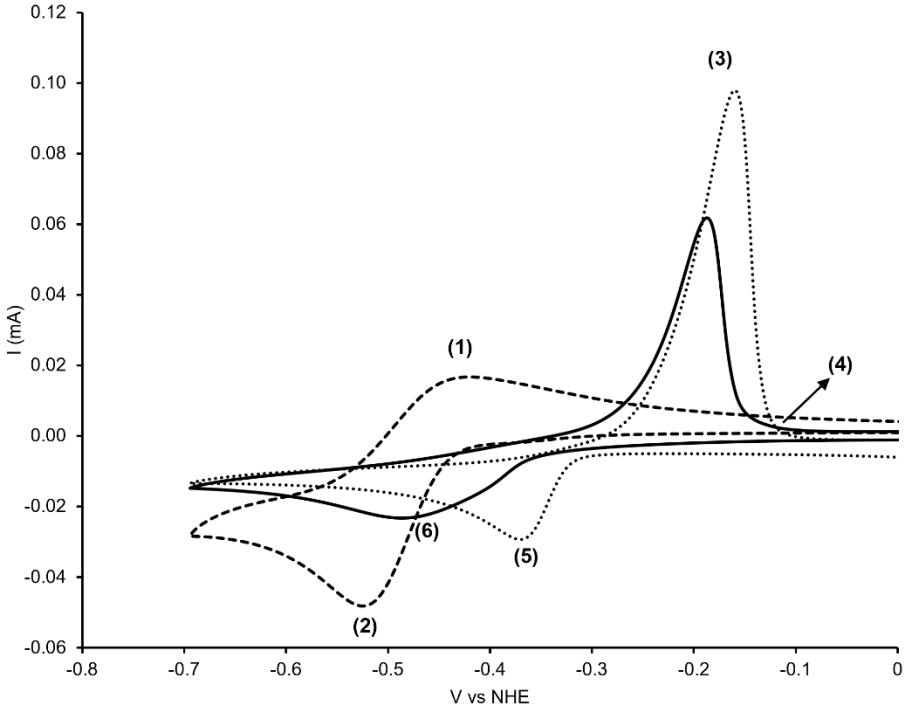

Figure S7. Cyclic voltammogram of Cu(Def)(py), $Cu(py)_4$ (dotted line), and blank (dashed line) in 25% pyridine (v/v): 75% 500 mM KCl (aq) (pH=7.4).

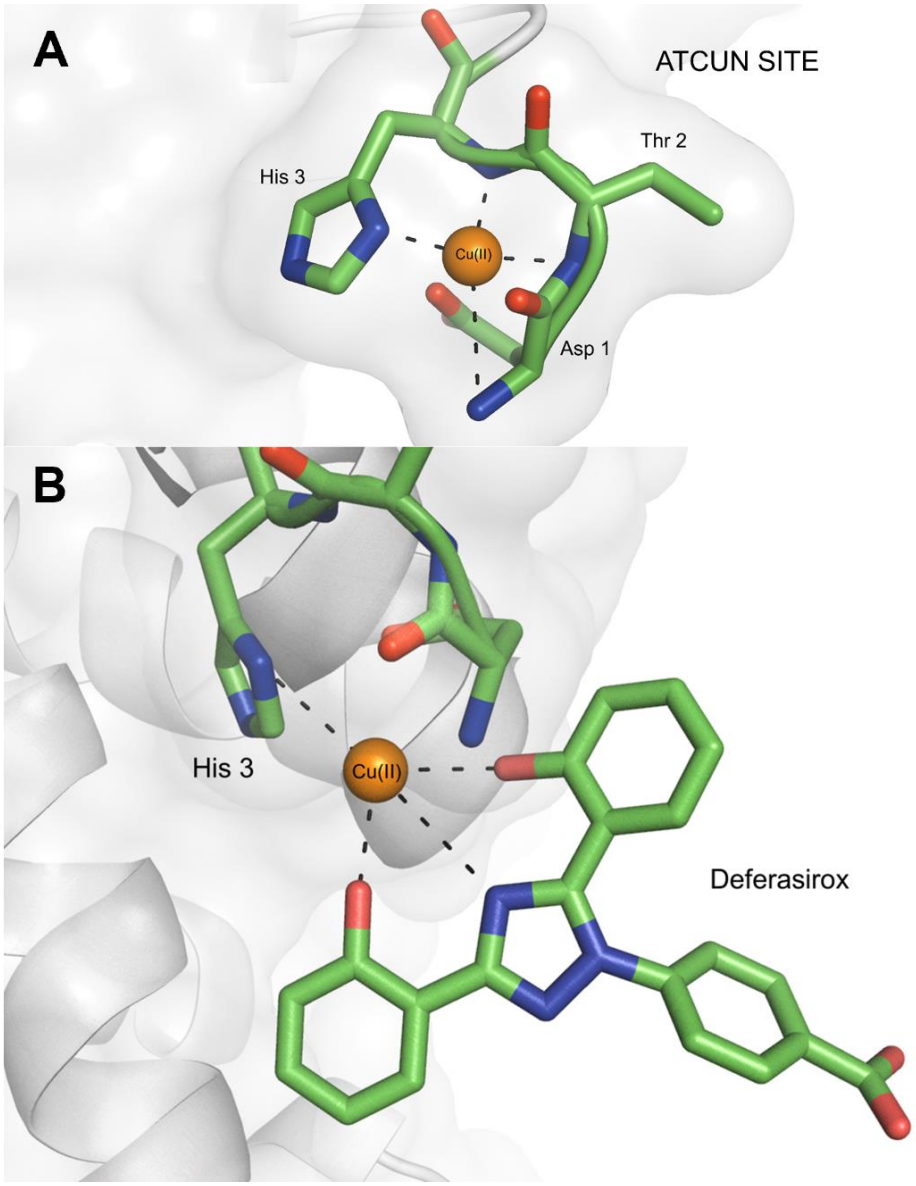

Figure S8. Cu(II) coordination at the ATCUN site of bovine serum albumin. (A) Cu(II) coordination in the classical modality (PDB 3V03). (B) Proposed model for the ternary Cu(BSA)(Def) complex. We required Def in a planar form for this model, and we resorted to our $Ti(Deferasirox)_2$ crystal structure (CCDC 2016873).[1] This crystal structure was modified to have only one Def structure. Once the planar Def structure was obtained, it was imported to the previously prepared Cu(II)-bound BSA file, and the Cu(II) was slightly translated to adopt a square planar arrangement.

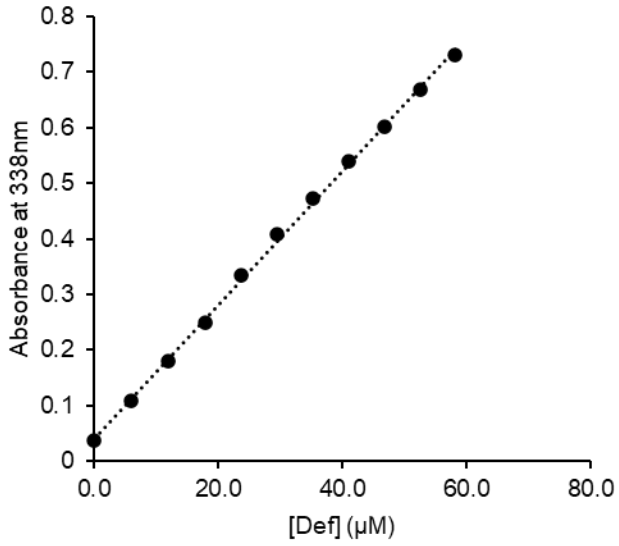

Figure S9. Titration of Cu(II)-bound BSA with Def to produce the Cu(BSA)(Def) ternary complex. The absorbance at 338 nm for the LMCT band was collected to determine the extinction coefficient from the line of best fit (y=0.01201x+0.04106).

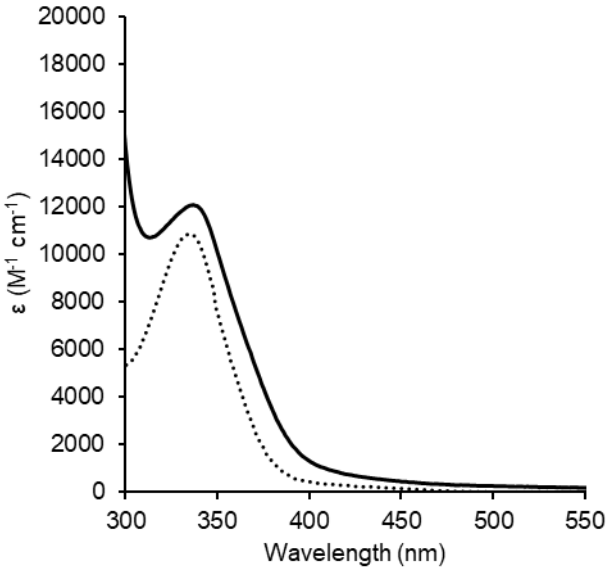

Figure S10. A comparison of the UV-Vis spectra of the ternary Cu(BSA)(Def) complex (black line) and Cu(Def)(py) (dashed line). The spectra are similar but not identical.

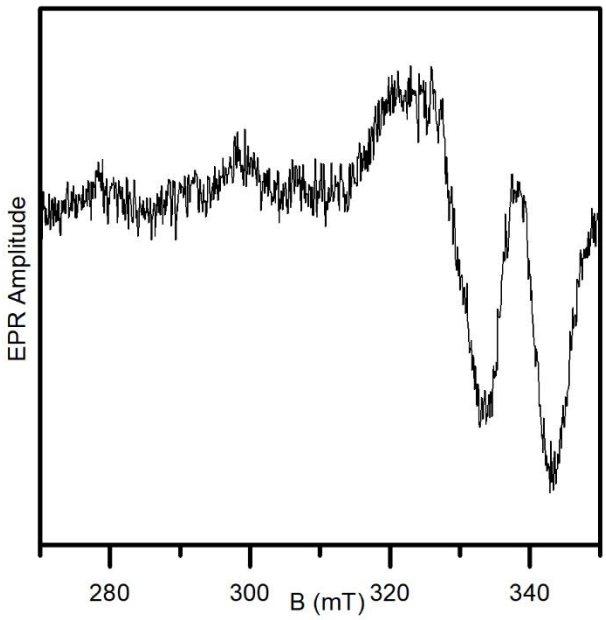

Figure S11. EPR Spectra of 500 μM Cu(II)-bound BSA and reacted with equimolar Def in frozen 50:50 (v/v) glycerol: 20 mM HEPES buffer (pH 7.4).

2. Supporting Table

Table S1. A summary of the NCI 60 cancer cell line viability screen against 10 μM of Cu(Def)(py) for 72h. The data were calculated as the mean per cell line type.

Cancer Cell Line Type	% Mean Cell Growth
Leukemia	68.7
Non-Small Cell Lung	102.9
Colon	81.3
CNS	75.3
Melanoma	38.4
Ovarian	80.4
Renal	88.1
Prostate	94.8
Breast	94.4

3. References

[1] K. Gaur, S. C. Perez Otero, J. A. Benjamin-Rivera, I. Rodriguez, S. A. Loza-Rosas, A. M. Vazquez Salgado, E. A. Akam, L. Hernandez-Matias, R. K. Sharma, N. Alicea, M. Kowaleff, A. V. Washington, A. V. Astashkin, E. Tomat, A. D. Tinoco, *JACS Au* **2021**, *1*(6), 865-878.